1996ApJ...463..747S

THE ASTROPHYSICAL JOURNAL, 463:747–765, 1996 June 1
© 1996. The American Astronomical Society. All rights reserved. Printed in U.S.A.

OPTICAL AND X-RAY CHARACTERISTICS OF STARS DETECTED IN THE *EINSTEIN* SLEW SURVEY[1]

JONATHAN F. SCHACHTER,[2,3] RON REMILLARD,[4] STEVEN H. SAAR,[2,5] FABIO FAVATA,[6]
SALVATORE SCIORTINO,[7] AND MARCO BARBERA[7]

Received 1995 January 11; accepted 1995 December 11

ABSTRACT

We detect X-rays for the first time from 63 cool (types A–M) stars. These stars are part of the 229 total stellar X-ray sources identified to date in the *Einstein* Slew Survey (hereafter Slew). We also list new X-ray data on one A star that *may* have a corona, five OB stars, and report discoveries of two new T Tauri stars and two new cataclysmic variables. The stellar content of the Slew high-latitude subset (currently 93% identified for $|b_{II}| > 20°$) is 26%. This agrees well with the *Einstein* Extended Medium Sensitivity Survey (EMSS) stellar sample, which only considered high latitudes. Because of the large solid angle covered by the Slew, and its shallow limiting flux, the sample will better probe the bright end of the stellar X-ray luminosity function ($L_X > 10^{30}$ ergs s^{-1}). Presently (based on the 221 Slew stars with known spectral types), the sample is dominated by late-type systems (cooler than F; 68%).

These include dMe's, BY Dra, RS CVn, and FK Comae systems. Based on the limiting magnitudes of catalogs searched to date, the Slew is assessed to be complete for spectral types earlier than K. Hence, K and M systems will be prominent in the $\sim$50 as yet unidentified stars.

We have embarked on an extensive program to (1) confirm the X-ray identifications with the optical counterparts; (2) search for Ca II H and K and Balmer line emission as activity signatures; and (3) search for supporting evidence of magnetic activity by measuring rotational velocities and relating them to X-ray luminosity level. Of 64 proposed coronal systems observed to date, we have confirmed 44 active stars, while in the remaining 20 we have been unable to find definitive activity. We have confirmed an additional 19 active stars from stellar database searches, and reclassified nine systems as having non-stellar optical counterparts from optical follow-up identification work and extragalactic database searches. We discuss notable new discoveries.

From the sample of single active F7–M5 Slew stars with measured $v \sin i$-values, we find a strong (99.9% confidence level) linear correlation of X-ray luminosity with $v \sin i$ and with stellar radius (R). However, L_X is uncorrelated with angular rotation speed at the 99% level. For the combined Slew and EMSS single star F7–M5 sample, we find the same 99.9% $v \sin i$–L_X and R–L_X correlations. The L_X–$v \sin i$ relation for the combined sample appears to flatten with respect to the quadratic behavior seen for optically selected stellar samples at rotational velocities in excess of $\sim$16 km s^{-1}. For the unevolved subset of the Slew single star sample, we also find a correlation between L_X and Rossby number (R_0; more than 99% confidence). A least-squares fit gives $L_X \sim R_0^{-0.4}$, which is similarly flatter than the quadratic dependence seen in optical samples. Using the stellar surface X-ray flux F_X versus $B-V$ diagram, we interpret these results as saturation of the stellar surface by active regions at $F_X/F_{bol} \approx 10^{-3}$.

Subject headings: stars: activity — stars: flare — surveys — X-rays: stars

1. INTRODUCTION

To date, stellar activity has been established in all stellar types except A (Vaiana et al. 1981; Rosner, Golub, & Vaiana 1985). Many of the most exciting discoveries benefited from the last decade of X-ray satellites, primarily *Einstein* and *EXOSAT*. Recent reviews of pre-*ROSAT* stellar observations can be found in Pallavicini (1989), Linsky (1990), Schmitt (1990), Vaiana (1990), Vaiana et al. (1992), and Sciortino (1993).

The large spread of L_X for stars of same spectral type and luminosity class clearly shows that "classical" stellar parameters cannot explain the wide range (several orders of magnitude) of X-ray activity seen among different members of a given spectral class. Since 1979, the stellar magnetic field has been proposed as a crucial ingredient to explain the coronal emission of cool stars (Rosner & Vaiana 1980). Its interplay with stellar rotation rate, spin-down with increasing stellar age, and depth of convection zone would result in stellar dynamos of varying efficiency. In this interpretational framework, the spread in the observed X-ray luminosities mainly reflects the differing efficiencies of stellar coronal heating. It is hypothesized that the heating mechanism is mainly due to the interaction between stellar magnetic fields and coronal plasma, a mechanism clearly at work on the Sun (although acoustic heating effects may also play a role; Ulmschneider 1990). X-ray data are thus

[1] Based on observations taken at the ESO La Silla observatory and Cerro Tololo Inter-American Observatory.

[2] High Energy Astrophysics Division, Harvard-Smithsonian Center for Astrophysics, 60 Garden Street, Cambridge, MA 02138.

[3] Visiting Astronomer at the National Radio Astronomy Observatory (NRAO), which is operated by Associated Universities, Inc., under contract with the National Science Foundation (NSF).

[4] Massachusetts Institute of Technology, Center for Space Research, Room 37-595, Cambridge, MA 02139.

[5] Visiting Astronomer, NSO, NOAO. NOAO is run by AURA, Inc., for the NSF.

[6] Astrophysics Division, European Space Agency, P.O. Box 299, 2200 AG, Noordwijk, The Netherlands.

[7] Istituto e Osservatorio Astronomico di Palermo, Palazzo dei Normanni, Palermo, Italy.

© American Astronomical Society • Provided by the NASA Astrophysics Data System

1996ApJ...463..747S

extremely useful, to measure the relation between X-ray luminosity L_X and the stellar rotational velocity ($v \sin i$), or between L_X and the Rossby number (R_0), either of which are thought to measure the strength of the putative dynamo. The dynamo generates magnetic fields, which confine and heat the corona. For optically selected samples (Pallavicini et al. 1981, 1982), $L_X \propto (v \sin i)^2$, providing the clearest evidence for magnetic processes. However, in samples of rapidly rotating stars both in the Pleiades (K stars; Caillault & Helfand 1985; Micela et al. 1985b, 1990; Stauffer et al. 1994) and the EMSS, the L_X–$v \sin i$ relation flattens at high values of $v \sin i$ ($\gtrsim 20$ km s^{-1}; Fleming, Gioia, & Maccacaro 1989). These results can be naturally interpreted as the existence of a saturation level in stellar coronal emission occurring when the entire stellar surface is covered with solar-like active regions (Vilhu & Walter 1987). Another possibility is that increased dynamo field generation eventually inhibits helicity, convection, differential rotation, or some combination, restricting further dynamo action and limiting the total magnetic flux generated (and the associated coronal heating) to some saturation value (Gilman 1982).

Other important questions include the turn-on and turn-off of coronal activity in stars with convective envelopes as a function of spectral type. The onset of coronal activity is thought to occur at or near F5 (Schmitt et al. 1985), although Altair (A7 IV–V) is an apparent exception (Golub et al. 1983). For earlier spectral types, magnetic effects may be due only to a residual primeval field; solar–like dynamos are not expected to exist due to a lack of a surface convective zone (L_X is uncorrelated with $v \sin i$; Pallavicini et al. 1981; Sciortino et al. 1990). *Einstein* IPC (Cash & Snow 1982; Schmitt et al. 1990; Micela et al. 1990; Grillo et al. 1992) and *ROSAT* PSPC (Drake et al. 1994a, 1994b; Schachter & Elvis 1994) observations have occasionally discovered both normal and chemically peculiar late-B/early-A stars. The main observed difference with the late–type systems is that in early–type stars there is a direct correlation between stellar mass and L_X (e.g., $L_X/L_{bol} = 10^{-6}$–10^{-7} for a wide range of O and B star types; Harnden et al. 1979; Sciortino et al. 1990). Given the limited spatial resolution of these observations, the X-ray emission either originates from unseen late-type companions or requires some alternative mechanism (Linsky 1985, 1993; Linsky, Drake, & Bastian 1992). The possible detections of X-ray emission from late-B stars having late–type PMS stars as companions in recent *ROSAT* HRI observations (Schmitt et al. 1993) call for further investigations; meanwhile, X-ray emission has recently been shown to be common in Herbig Be B stars (Damiani et al. 1994; Zinnecker & Preibisch 1995).

1.1. *The Slew Sample of Coronal Stars*

To resolve these and other key questions about coronal processes uniformly selected samples of stellar sources are required. Of particular interest is the bright tail of the X-ray luminosity functions of active stars, providing many good examples for follow-up work and analysis, since stars are typically among the most X-ray quiet (i.e., low X-ray-to-optical flux ratio) sources. These X-ray luminous stars are the major contributors to the stellar X-ray number counts and may account for more than 50% of the 1.15–2 keV background at low Galactic latitudes (Kashyap et al. 1992; Sciortino 1993; Sciortino, Favata, & Micela 1994).

We have therefore searched (via optical tests for chromospheric emission lines) for coronally active stellar counterparts to X-ray sources in the Slew, a flux-limited ($\sim 3 \times 10^{-12}$ ergs cm^{-2} s^{-1}, 0.2–4.0 keV) all-sky ($\sim 36{,}000$ deg^{-2}) survey constructed from the slewing observations of the *Einstein* IPC (Elvis et al. 1992; Plummer et al. 1994). There are 809 sources in the Slew, with a false source rate of 2%, and a positional accuracy of 72″ at 90% confidence (120″ at 95% confidence).

To place the Slew in the context of other IPC sky surveys, we can compare it with the *Einstein* Extended Medium Sensitivity Survey (EMSS; Stocke et al. 1991), the *Einstein* Galactic Plane Survey (GPX; Hertz & Grindlay 1988), and the *Einstein* optically selected stellar survey (Vaiana et al. 1992; Sciortino 1993, and references therein). All of these are biased toward sources $\sim$3–10 times fainter than typical Slew sources because of the small areas: the EMSS covers only 780 deg^2 of sky (and only for $|b| > 20°$), the GPX covers 185 deg^2 (and only for $|b| < 15°$). The *Einstein* optically selected stellar survey, based on the full set of *Einstein* pointings, covers $\sim$3000 square degrees. Since the Slew covers all latitudes, it will not be biased against low scale height stars (e.g., O and B stars) as was the EMSS (e.g., Table 4-16 of Mihalas & Binney 1981). The larger solid angle covered by the Slew better probes the bright end of the stellar X-ray luminosity function ($L_X > 10^{30}$ ergs s^{-1}; e.g., Fig. 4 of Sciortino 1993), covered only sparsely by previous *Einstein* surveys.

We will now use the EMSS-derived X-ray-to-optical flux ratios ($-5.5 \leq f_X/f_V \leq 0.0$; Vaiana et al. 1992) to aid in the optical identification of the Slew stars by predicting their V-magnitudes. The expected average V-magnitudes by spectral type are $V = 5.8$ (B stars), $V = 5.7^{+1.3}_{-2.0}$ (F stars), $V = 7.2^{+1.5}_{-2.0}$ (G stars), $V = 9.0^{+1.7}_{-3.5}$ (K stars), and $V = 10.5^{+2.2}_{-1.3}$ (M stars). Here, we have given 1 σ ranges robustly defined by with 16% and 84% sextiles, except for B stars, where only four were detected in the EMSS. These predictions are essentially independent statements about the Slew Survey, whose stellar sample has little overlap with that of either the EMSS or GPX (e.g., only seven Slew stars in the EMSS).

The additional deviation expected from the spread in the Slew flux distribution is small by comparison (-0.7, $+0.6$ mag). We discuss the observed magnitude distributions of Slew stars, by spectral type, and the f_X/f_V-values of individual sources in § 2.2.

To verify these predictions, to discover new interesting objects, and to build an independent X-ray selected sample to address the various open issues of stellar coronal physics, we have undertaken an extensive identification program of the stellar content of the Slew (as a part of the ongoing general identification program of Slew sources). The Slew can be used to search for very rare, very active stars that would otherwise be undetected by optical surveys, thus probing the large spread in L_X for stars of the same spectral type. It can test the effects of magnetic activity and convection on X-ray emission by correlations between L_X and intrinsic stellar parameters, and it can probe the onset of coronal activity by searching for emission from A stars.

Here we report results of this effort that has started through extensive literature searches to find stars in the X-ray error circles (e.g., by querying stellar databases) and then continued through optical spectroscopy to confirm their identifications as optical counterparts.

© American Astronomical Society • Provided by the NASA Astrophysics Data System

1996ApJ...463..747S

A description of the sample selection is provided in § 2, which includes the combined technique of positional coincidences and follow-up optical spectroscopy. This is followed by a discussion of the correlations of other stellar parameters with L_X in both the single star and binary star samples, and the implications for rotational saturation (§ 3). We summarize in § 4.

2. OBSERVATIONS, METHODS, AND RESULTS

2.1. *Positional Coincidences from Stellar Databases*

Since many of the Slew stars were expected to be bright, we first searched stellar catalogs and databases for sources within the X-ray error circles. However, since published optical positions can have errors, we used a conservative 180″ radius to search for positional coincidences. All sources falling within each search radius were retained.

Complementary optical identifications work for nonstellar sources is described in Elvis et al. (1992), Schachter et al. (1993), and Perlman et al. (1996). We searched large stellar catalogs (Bright Star Catalog, SAO, HD), providing completeness down to $V \sim 8$. Using the expected magnitudes from the previous section, we see that magnitude-limited catalog searches will selectively miss some of the K and M stars, but should find all of the B, F, and a large fraction of the G stars. To go fainter in V, we used the distance-limited Gliese and Woolley catalogs. We could conceivably have used the Hubble Guide Star Catalog (GSC; limiting $V \approx 14$). However, the GSC provides no spectral type information (essential for picking out suspected coronal sources), coarsely estimated magnitudes with uncertainties in the range 0.3–0.5 mag, and suffers from a huge chance coincidence rate because of the high spatial density (counterparts in more than 50% of Slew error circles). We note that any faint stars (say, $V > 12$) must therefore be carefully scrutinized. To go fainter than the SAO and HD catalogs, we queried the SIMBAD stellar database. SIMBAD also provided up-to-date magnitudes and spectral types, and reported nonstellar sources in the error circle.

In this search process, we found a total of 246 Slew sources with stellar positional coincidences. Of these, 164 are already cataloged as X-ray sources (Elvis et al. 1992, and references therein), generally confirming the identification of the Slew source with the proposed optical counterpart (but see notes to tables for our corrections to X-ray identifications in the literature). For the remaining 82 stars with no X-ray detection previous to the Slew, we have begun a comprehensive observing program (details in the following section) to confirm the identifications.

Before discussing the various techniques we have adopted to confirm the proposed catalogs identifications, we need to quantify the chance coincidence rate in Slew error circles. From the SAO catalog (complete to $V \approx 8$), we expect four chance SAO stars *within the* 3′ *radius error circles* for the 82 Slew stars with no previous X-ray detection. Note that this estimate is conservative, as we are using a very generous error circle. In fact, 55 of these 82 have SAO counterparts. The rest are approximately half $V = 9$–10 stars (i.e., just below the SAO catalog completeness), and half $V > 10$ stars, both groups gleaned from SIMBAD.

2.2. *Checking the Coincidences: X-Ray Properties*

Without doing any observing, we can already show that the majority of the positional coincidences are, in fact, correct X-ray identifications. We have inspected the magnitude distributions for each spectral type of Slew stars (both previously known and previously unknown X-ray sources) and find that they are in general non-Gaussian, with broad wings and (for the G and K stars) bimodality (Fig. 1). Comparing these results to those of § 1, we find that the distributions of optical magnitudes are very similar to that expected from the f_X/f_V-values in the EMSS. In other words, the Slew stars have reasonable values of f_X/f_V. Of course, in any given star there will always be variations in f_X/f_V produced by variations in activity, and the nonsimultaneity of Slew and optical observations. This emphasizes the need for complete, uniformly selected, stellar samples, to average out the single source variability.

We focus now mainly on the stars that were found, via positional coincidences, to lie within Slew error circles, and yet have no previously reported X-ray detection (except for a few early published results from *ROSAT*). These stars are tabulated in Table 1. Part A of Table 1 contains stars that we believe are associated with the X-ray source and possess observable signs of activity, or have not yet been observed to confirm activity. Some 63 of these are cool stars (spectral types A–M). Part B of Table 1 contains stars in which our observations have not been able to find any sign of activity. However, nearly all have reasonable values of f_X/f_V. Further optical observations are needed to resolve these cases. A small number of the Slew sources for which we had proposed new stellar X-ray identifications (Table 7 of Elvis et al. 1992) have subsequently been found to have nonstellar counterparts. These are noted in Table 2. Also see updates to proposed nonstellar identifications in Plummer et al. (1994).

In part A of Table 1, we summarize the relevant information and criteria used to verify the association between the X-ray detection and the proposed stellar identification in each case. For most of the stars in the sample (part A of Table 1), optical magnitudes are known, so verifying f_X/f_V (col. [5]) is done first. In the majority of cases, the f_X/f_V-values are within the ranges found for EMSS stars (Sciortino et al. 1993): $\log f_X/f_V = -4.6$ to -3.0 for B stars -5.0 to -2 for F stars, -5.5 to -2.0 for G stars, -4.0 to -1.5 for K stars, and -3.1 to -0.0 for M stars. We note with a question mark (?) in column (5) cases where the f_X/f_V-value falls nominally outside these ranges. The notation "G?" means, for instance, that the spectral class of G may be incorrect, but a stellar identification is still plausible. There are only 2 known cases where the observed f_X/f_V lies significantly outside the range of stellar coronal sources: 1ES 0437−046 (a new cataclysmic variable) and 1ES 1841−044 (another probable accretion-powered source). These cases are noted by an "X" in column (5); see § 2.5 for more details.

We have compiled X-ray data (mainly *Einstein* upper limits and as yet unreported new *ROSAT* detections) to provide additional evidence—either from the literature, or, for the case of the *ROSAT* survey, in separate work we have done at MPE (Schachter, Elvis, & Voges 1993)—that the stellar identification with the Slew source is correct. All the available evidence has been used, since discounting the identification is always easier than confirming it. Indeed, we find that identifications proposed in the literature of X-ray sources with stars are incorrect in a few (∼5) cases (Table 5 below), as they have been based simply on a positional coincidence within the X-ray error box. We have found two

© American Astronomical Society • Provided by the NASA Astrophysics Data System

1996ApJ...463..747S

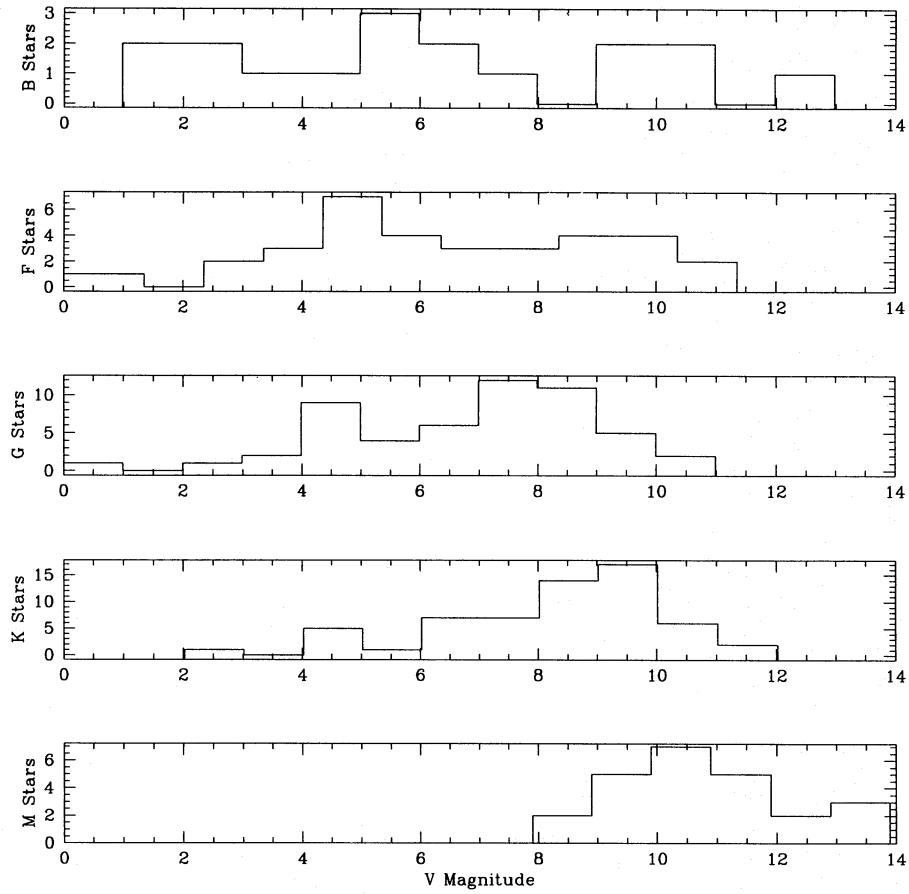

FIG. 1.—Distributions of observed V-magnitudes for all 246 stellar identifications in the Slew Survey, by spectral type, using bins of 1 mag. The median observed magnitudes and the 16% and 84% sextiles are B stars at $5.6^{+5.1}_{-3.5}$, F stars at $6.1^{+3.3}_{-2.2}$, G stars at $7.3^{+1.4}_{-2.7}$, K stars at $8.7^{+1.3}_{-2.4}$, and M stars at $10.6^{+1.9}_{-1.6}$. These are in agreement with the numbers predicted by the X-ray-to-optical flux ratios (§ 1.1): $V = 5.8$ (B stars), $V = 5.7^{+1.3}_{-2.0}$ (F stars), $V = 7.2^{+1.5}_{-2.0}$ (G stars), $V = 9.0^{+1.7}_{-3.5}$ (K stars), and $V = 10.5^{+2.2}_{-1.3}$ (M stars).

kinds of these cases: (1) another star in the error circle is a more likely optical counterpart than the one previously reported, and (2) the X-ray source is composite (two or more stars). This illustrates the need to search for optical confirmations of activity.

2.3. *Checking the Coincidences: Optical Observations*

Stellar activity was confirmed by our program of low-resolution optical spectroscopy. We relied on detectable Ca H and K (and perhaps Balmer) emission, or filled-in absorption. We also searched for magnetic signatures of enhanced magnetic dynamo activity. Rapid rotation is strongly correlated with chromospheric (e.g., Noyes et al. 1984) and coronal (Pallavicini et al. 1981) emission, and magnetic flux (e.g., Saar 1991) in cool stars, and hence observation of a high $v \sin i$ ($\gtrsim 10$ km s^{-1}) in a star provides a strong indication of significant activity.

A flowchart summarizing our basic observational approach is given in Figure 2. We divided the task of observing the stars in Table 1 into northern and southern groups. No precise declination cut was used, to provide overlapping observations of equatorial sources, which provide independent checks of the approaches. Instead, we take *northern* to mean observable from southern Arizona (Kitt Peak or Mount Hopkins) and *southern* to mean observable from Chile (Cerro Tololo or La Silla). Most northern observations were performed by R. R. and S. H. S., most southern observations by F. F., M. B., and S. S. Observational details are given in Table 3.

For technical reasons, both emission lines or large rotational velocities cannot be looked for in every star. Measurement of smaller $v \sin i$-values ($\lesssim 10$ km s^{-1}), requiring an echelle spectrograph, is usually possible only for brighter stars ($V < 11$ or 12). In the low-resolution work, the contrast of emission line cores (e.g., Ca H and K) relative to the photospheric absorption is more pronounced, and therefore more easily discovered, in late-type stars (K and M).

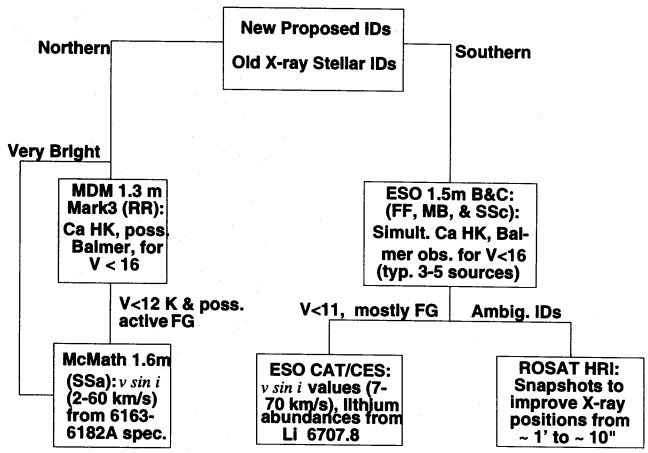

FIG. 2.—Flow chart of Slew stellar identifications procedure. See description in text.

© American Astronomical Society • Provided by the NASA Astrophysics Data System

1996ApJ...463..747S

TABLE 1

NEW STARS: X-RAY CONFIRMATIONS, ACTIVITY INDICATORS, AND NONCONFIRMATIONS

1ES Name (1)	Other Name (2)	Type (3)	V (4)	log f_X/f_V (5)	Other X-Ray Detections (Marginal)[a] (6)	Activity Indicators[a] (7)
			A: Confirmed Stars			
1ES 0013+195.....	G 32−6[b]	M4	13.00	−0.90	RASS	J. S.: dMe
1ES 0120+004.....	HD 8358	G0	8.40	−2.66 G	...	RS CVn (DSL92)
1ES 0143−253.....	HD 10830	F2 IV	5.31	−3.95	...	binary (C84), FBS: 84 km s^{-1}
1ES 0154−518.....	HD 11937	G8 IV	3.70	−3.98	RASS	Ca II (PP91)
1ES 0157+706.....	NSV 694	F2 V	6.77	−3.46	...	S. H. S.: 10 km s^{-1}
1ES 0226−615.....	HD 15638	F3 IV/V	8.70	−2.31 F?	...	FBS: 62 km s^{-1}
1ES 0237−531[c].....	HD 16699	F8 IV/V	7.00	−2.78	...	FBS: 20 km s^{-1}
1ES 0238+057[c].....	BD +05 378	M	10.57	−1.98	...	FBS? Hα, 4.4 km s^{-1}
1ES 0305−284[c].....	GJ 1054A	K7 V	10.20	−1.95	...	FBS: 30 km s^{-1}
1ES 0309−291.....	HD 20010	F8 IV	3.85	−4.00	...	Ca II (PP91)
1ES 0324+095[c].....	HD 21364	B9 Vn	3.74	−4.32	*ROSAT* WFC	FBS
1ES 0357−400[c].....	HD 25300	K0	9.90	−2.11	...	FBS: 12 km s^{-1}
1ES 0412+060[c].....	HD 26913	G5 IV	6.31	−3.82	(2 σ, W80)	FBS: 6.3 km s^{-1}, RS CVn (DSL92)
1ES 0415+231.....	HD 284303	K0	9.56	−2.18	*ROSAT*, St92	BY Dra (Dr93)
1ES 0415+283.....	V 410 TAU	K5	11.85	−1.40 K?	*ROSAT*, St92	PMS; weak Ca II (HP92)
1ES 0423+146.....	HD 27836	G7 III	4.90	−4.55	*ROSAT*, St92	chrom. em.? (Du84)
1ES 0426−131.....	HD 28497	B2 Vne	5.60	−4.23	(U.L., LW80)	Hα(GR85)
1ES 0429+130.....	HD 286839	K0	11.00	−1.85	*ROSAT*, St92	chrom. activ. (St91)
1ES 0437−046.....	BF ERI	B0	13.50	−0.05 X	...	FBS, R. R.: CV
1ES 0437+444.....	BSD 24−491	...	10.78	−0.79	...	Hα (CM83)
1ES 0444−704[c].....	HD 270712	K7	...	...	...	FBS: dKe, 11 km s^{-1}
1ES 0447+068[c].....	HD 30652	F6 V	3.30	−4.34	...	Ca II (P89), FBS: 16 km s^{-1}
1ES 0504−575[c].....	HD 33262	F7 V	4.71	−3.79	...	Ca II (PP91), FBS: 12 km s^{-1}
1ES 0510−119[c].....	SAO 150223	B8 V	4.50	−4.26	...	FBS: 14 km s^{-1}
1ES 0603−484[c].....	HD 41824	G6 V	6.57	−3.00	RASS	FBS
1ES 0635−698[c].....	HD 47875	G3 V	...	...	...	FBS: 10 km s^{-1}
1ES 0637−614.....	HD 48189	G0 V+G8 V	6.18	−3.33	...	FBS: 15 km s^{-1}, bin.
1ES 0738+612[c].....	HD 61396	K0	8.10	−2.38	...	R. R., radio src (B91)
1ES 0740+228.....	SAO 079647	K0	10.00	−1.93	...	R. R., S. H. S.: 17.0 km s^{-1}
1ES 0829+159.....	MCC 527	K8	10.17	−1.73	...	R. R.
1ES 0919+404.....	HD 80715	K3 V+K3 V	7.70	−2.54	...	S. H. S., BY Dra (St88)
1ES 0920−136.....	HD 81032	K0 IV	8.50	−2.35	...	R. R.
1ES 0957+247.....	HD 86590	K0 V	7.90	−2.40	(2 σ, W87)	RS CVn (B81, DSL92)
1ES 1002−559[c].....	HD 87525	K1–2 III	7.90	−2.76	...	FBS: 16 km s^{-1}
1ES 1105+833.....	SAO 18249	K2	9.90	−1.40 K?	...	R. R. (SE star)
1ES 1126−610[c].....	HD 306536	A	10.00	−1.97 F?	...	...
1ES 1228−465.....	HD 108866	F5 V	8.70	−2.34 F?	RASS	...
1ES 1239−011.....	HD 110379	F0 V	3.7	−4.52	RASS (U.L., Sc85)	...
1ES 1252−060[c].....	GJ 488.2	K8 V	10.27	−2.36	...	R. R., FBS: 7.5 km s^{-1}
1ES 1301−411[c].....	CD-40 7655	K0	10.00	−2.09	RASS	...
1ES 1314+172[c].....	HD 115404	K2 V+M2 V	6.50	−3.46	...	Ca II (V78)
1ES 1339−688[c].....	HD 119022	G2 IV/V	7.7	−2.57	...	FBS
1ES 1354−314.....	HD 121688	K0 V	10.60	−1.97	...	R. R., S. H. S.: 63 km s^{-1}
1ES 1456−400.....	HD 132349	F7–F8 V	10.40	−1.52 F?	...	J. S.: Ca II?
1ES 1509+763.....	HD 135363	G5	9.20	−2.23	...	R. R.
1ES 1614+446.....	HD 146696	G0	8.70	.632	...	R. R.?, S. H. S.: 65 km s^{-1}
1ES 1650−417.....	HD 152219	O9 IV	9.40	−2.71	(U.L., CHS89)	...
1ES 1727+590[c].....	HD 159023	G0	8.10	−2.67	RASS	R. R.
1ES 1737+612.....	AC +61 27026	K8 V	10.3	−2.07	WFC	R. R.
1ES 1746+748.....	SAO 8910	K0	10.00	−2.27	...	R. R.
1ES 1824+151.....	HD 170052	K0	8.73	−1.99	...	R. R., S. H. S.: 17 km s^{-1}
1ES 1833+169.....	HD 171746	G2 V+G2 V	6.21	−3.84	RASS	S. H. S.: 5 km s^{-1}
1ES 1841−044[c].....	FT SCT	...	16.65	0.72 X	...	...
1ES 1902−524.....	HD 177171	F7 V	5.16	−3.44	RASS	...
1ES 2013+448.....	HD 192785	K0	8.10	−3.08	...	R. R., S. H. S.: SB2, 12 km s^{-1}
1ES 2048+314[c].....	SAO 70569	K0	9.10	−2.50	RASS	...
1ES 2052+441.....	HD 199178	G2 V	7.60	−2.51	...	FK Com (PV82)
1ES 2058+398[c].....	GJ 815ABC	M3e V+M3e V	10.10	−1.90	...	Hα (SH86)[g]
1ES 2128+231.....	BD +22 4409	K8	9.25	−2.19	...	R. R., Ca II (G80)
1ES 2153+441.....	HD 208472	K0	7.40	−2.82	...	S. H. S.: ~18 km s^{-1}
1ES 2155−081.....	BD-08 5773	...	9.50	−2.64	RASS	J. S.: Ca II?
1ES 2216+845.....	SAO 3717	K2	9.70	−2.22	...	R. R.
1ES 2257−340[c].....	HD 217344	G5 Vp	8.60	−2.46	...	Ca II (St88), FBS: 72 km s^{-1}
1ES 2326+411[c].....	G 190−28	dM2e	13.40	−0.61	...	R. R.: Hα
1ES 2347+485.....	AG +48 2130	F5	9.90	−1.99 F?	...	...

© American Astronomical Society • Provided by the NASA Astrophysics Data System

1996ApJ...463..747S

TABLE 1—*Continued*

1ES Name (1)	Other Name (2)	Type (3)	V (4)	log f_X/f_V (5)	Other X-Ray Detections (Marginal)[a] (6)	Activity Indicators[a] (7)
			B: Unconfirmed Stars			
1ES 0419+148.....	HD 285758	F8	10.00	−2.71	...	...
1ES 0618−580.....	HD 44627	K2 V	9.10	−2.39	...	...
1ES 0712−363.....	HD 56142	F6–7 V	7.40	−2.94	...	...
1ES 0717−572.....	HD 57555	G0 IV/V	7.90	−2.71	...	...
1ES 1020+493.....	HD 89944	F5	8.70	−2.67	...	...
1ES 1318−632.....	LS 3039	B	12.80	−0.74 X	...	...
1ES 1325−261.....	HD 117033	K5 III	6.70	−3.64	...	...
1ES 1326+789.....	HD 117566	G2.5 IIIb	5.77	−3.66	...	...
1ES 1327−313[d].....	HD 117310	K1 III	9.6	−2.48	...	...
1ES 1414−197.....	HD 125048	A5 IV	6.90	−3.38	...	...
1ES 1414+203.....	HD 125040	F8 V	6.25	−3.60	...	...
1ES 1437−252.....	HD 129009	F0–2 V	9.40	−1.88 F?	...	...
1ES 1606+218.....	BD +22 2931	K2	10.90	−1.99	...	...
1ES 1711−547.....	HD 155573	F0 IV/V	9.50	−2.15 F?	...	...
1ES 1716+551[e].....	HD 156984	K0	7.70	−3.15	...	...
1ES 1914+092.....	HD 180660[b]	K2 IIvar	8.50	−3.00	...	...
1ES 1920+223.....	HD 344230	A2	10.00	−1.83 F?[f]	...	...
1ES 2001+068.....	HD 190342	K2	9.20	−1.80	...	...
1ES 2042+335.....	SAO 70451	G5	9.30	−2.83	...	...
1ES 2135+011.....	AG +01 2623	K0	10.40	−2.09	...	...
1ES 2129−026.....	PHL 26	...	18.60	1.23 X	...	...
1ES 2334+063.....	HD 221973	G0	8.60	−2.61	...	...

NOTES.—1ES 0237−531: There are two stars within 1′ in the error circle, with similar late F B&C spectra. One has high Li, the other is a fast rotator. No clear cut identification. 1ES 0238+057: Although this star was reported as a dM0 in Robertson & Hamilton (1987), we find it to be of slightly earlier spectral type (mid-K). It has strong Ca II H and K and Hα emission, and a weak Li I line (15 mÅ) and hence is apparently a typical dKe. 1ES 0305−284: Strong Ca II H and K, and Hα emission, very fast rotator. 1ES 0324+095: On edge of *ROSAT* Wide Field Camera error circle. Optical counterpart is an ambiguous ID, very bright. 1ES 0357−400: Easily visible Ca II H and K emission cores, and Hα emission, fairly strong Li I absorption (100 mÅ). Perhaps a Pleiades-age star. 1ES 0412+060: The Slew error circle also contains HD 26923 (a known X-ray source; Schmitt et al. 1990). 1ES 0444−704: Filled in Ca II, Hα in emission. 1ES 0447+068: Has a fainter companion, which could not be observed because of the strong glare of the primary. Known binary (Hartkopf & McAlister 1984). 1ES 0504−575: Companion present. 1ES 0510−119: Has a G8 Ve companion. Both appear to emit in X-rays, based on *ROSAT* HRI observations (Schmitt et al. 1992). 1ES 0603−484: No obvious signs of activity. Suspicious ID, high f_X/f_V. 1ES 0635−698: Two stars in error circle, both plausible counterparts. Brighter (HD 47875) is a G3 V with high Li I (200 mÅ), likely to be a quite young star. The fainter one is not in any catalog, and we classify it as K4 Ve. It has both Ca II H and K and Hα in emission. We have not obtained a Li I spectrum, but the Li I line appears to be visible in the low-resolution spectrum, implying an equivalent width of about 200 mÅ. 1ES 0738+612: Possible RS CVn (§ 2.4). 1ES 1002−559: An SB2 K-type giant system in which two similar spectral line systems are clearly visible in the high-resolution spectrum. The relatively high rotational velocity, together with the presence of Ca II H and K emission cores clearly visible in the low-resolution spectra, make this a previously undetected RS CVn type system. 1ES 1126−610: Quoted magnitude is B band, not V. As there are no A stars in the EMSS sample, we have compared the f_X/f_V-value of the proposed identification to that of F stars in the EMSS. 1ES 1252−060: Hα filled in. 1ES 1301−411: Outside 2′ Slew error circle (95% confidence), but within RASS error circle. 1ES 1314+172: Claimed (Dr93) as a BY Dra, but unlikely, as the system is a visible binary, and thus not close enough for tidal locking. 1ES 1339−688: Two normal looking G stars in the error circle, and an early M star with weak Hα emission. M star is the more likely ID. 1ES 1727+590: Ambiguous ID. Quoted magnitude is B band, not V. 1ES 1841−044: A low Galactic latitude variable star, possibly accretion powered. 1ES 2048+314: On edge of RASS error circle. 1ES 2058+398: A dMe spectroscopic triplet, was called WLY 815AB in Elvis et al. 1992; a BY Dra system (Dr93). 1ES 2257−340: RS CVn (DSL92). 1ES 2326+411: There are three other possible candidates in the error box, even using the RASS and Slew error circles together.

Col. (7) references are as follows. B81: Bolton et al. 1981. B91: Becker et al. 1991. C84: Corbally 1984. CHS89: *Einstein* upper limit (Chlebowski et al. 1989). CM83: Coyne & McConnell 1983. Dr93: Drake 1993. Du84: Duncan et al. 1984. DSL92: RS CVns (Drake et al. 1992). G80: Glebocki et al. 1980. GR85: Goraya & Rutela 1985. HP92: Hamann & Persson 1992. LW80: *Einstein* hot star survey upper limit (Long & White 1980). M90: Maggio et al. 1990. RASS: *ROSAT* all-sky survey (Schachter et al. 1993). WFC: *ROSAT* Wide Field Camera catalog (Pounds et al. 1993). P89: Pasquini et al. 1989. PP91: Pasquini & Pallavicini 1991. PV82: Piirola & Vilhu 1982. Sc85: *Einstein* upper limit (Schmitt et al. 1985). SH86: Stauffer & Hartmann 1986. St88: Strassmeier et al. 1988. St91: (Stauffer et al. 1991). St92: *ROSAT* Hyades survey (Stern et al. 1992). V78: Vaughan et al. 1978. W87: *HEAO 1* 2 σ upper limit (Walter et al. 1987). W80: *HEAO 1* 2 σ detection (Walter et al. 1980).

[a] R. R.: confirmed by R. Remillard at MDM 1.3 m. S. H. S.: confirmed by S. Saar at McMath-Pierce. FBS: confirmed by F. Favata, M. Barbera, and S. Sciortino at ESO. J. S.: confirmed by J. Schachter at MMT or CTIO. All quoted velocities are values of $v \sin i$. Ca II emission is detected as an indicator of activity in cases where one or more of the authors initials are included without further elaboration. "Ca II" and "Hα" denote line emission cited in the literature. RASS: detected in our *ROSAT* all-sky survey work; see text. U. L.: upper limit.

[b] Multiple possible optical counterparts (see Elvis et al. 1992).

[c] See notes.

[d] Also see Fig. 3.

[e] S. Saar: $v \sin i = 5$ km s^{-1}.

[f] We have compared the f_X/f_V-value to that of EMSS F stars, as there are no A star detections in the EMSS.

© American Astronomical Society • Provided by the NASA Astrophysics Data System

1996ApJ...463..747S

TABLE 2

UPDATED NONSTELLAR IDENTIFICATIONS

1ES Name	Old ID	Old Type	New ID	New Type
1ES 0614+227.....	HD 254475	K2	IC 443	supernova remnant
1ES 0839−445.....	HD 74209	A0	Vela	supernova remnant
1ES 1101−606.....	SAO 251235	M0	MSH 11 − 61A	supernova remnant
1ES 1212+078.....	SAO 119284	K0	...	BL Lac[a]
1ES 1212−652.....	HD 106392	G0–G1 V	G299.2−2.9	supernova remnant[b]
1ES 1148−624.....	HD 309207	B8	G296.1 − 0.5	supernova remnant
1ES 1325−312.....	SAO 204500	F5 V	Shapley 8	galaxy cluster
1ES 1702+457.....	SAO 046462	F8	...	active galaxy[c]
1ES 1735−269.....	IRAS 17345−2656	...	...	*IRAS* source

[a] Identified in Perlman et al. 1996.

[b] Both 1ES 1212−151 and 1ES 1212−152 are now identified with the extended emission in this source; Slane et al. 1995.

[c] Identified as part of our nonstellar identification program.

2.3.1. *Approach for Northern Observations*

Beginning in 1991 June, one of us (R. R.) searched for Ca H and K emission (or cases of partly filled-in Ca H and K absorption) in medium-resolution (3 Å FWHM) spectroscopy at the Michigan-Dartmouth-MIT 1.3 m Telescope (Mark 3 Spectrograph) on Kitt Peak.[8]

For each field, the proposed optical counterpart based on our database searches was observed first at Ca H and K. If this star displayed clear signs of activity, it was then observed over a wider wavelength range to search for Hβ and Hα emission. Then the next field on the list was observed. If the star did not display clear signs of activity, other stars in the vicinity of the first star were observed at Ca H and K, typically down to $V = 16$. We provide examples of clear Ca H and K emission and filled-in absorption in Figure 3.

We list confirmed stars with the notation "R. R." in Table 1 (also see § 2.5).

Of the remainder, the bright ambiguous cases and confirmed active stars were passed on to another one of us (S. H. S.) for determinations of rotational velocity (v sin i) at the NSO McMath-Pierce 1.6 m echelle on Kitt Peak ($\lambda/\Delta\lambda = 125{,}000$). Very bright stars (third or fourth magnitude) and stars with Ca emission already reported in the literature were passed on as well. All the observations were inserted into a program of studying signatures of stellar magnetic activity in the spectral range 6163–6182 Å, which also provides a number of strong, relatively unblended lines for v sin i determinations.

Typical rotational velocity measurements are shown in Figures 3*f*, 3*g*, and 3*h*. Two basic methods were used. When v sin i was relatively low ($\lesssim 15$ km s^{-1}, e.g., Fig. 3*f*), lines were modeled with a simple LTE line transfer code, disk-integrated using 900 equal projected area sectors at 15 limb angles plus a radial-tangential macroturbulence (ζ) model (see Saar, Nordström, & Andersen 1990). Macroturbulent values were assumed from the mean ζ-spectral type relations given in Gray (1988) when S/N of the data was low, or fit separately when S/N $\gtrsim$ 200. When v sin $i \gtrsim 15$ km s^{-1} (e.g., Fig. 3*g*), a low v sin i star of approximately the same spectral type was convolved with a rotational broadening function (Gray 1988) until an optimal match to the data was achieved.

2.3.2. *Approach for Southern Observations*

After the northern identification follow-up program was started, three of us (F. F., M. B., and S. S.) initiated a dedicated program of ESO observations, beginning in 1992 December, as follows:

With the ESO 1.5 m Boller & Chivens (B&C) spectrograph, we searched for stellar activity, such as emission cores in Ca II H and K lines, or filled-in absorption or emission in Balmer series lines. The large 2048^2 CCD at the B&C enables sufficient resolution to search for Ca H and K emission cores in the late spectral types, and wide enough spectral coverage to get Hα. We show examples of emission and partly filled-in (or disrupted) absorption in Figure 4.

Typically, all sources within the Slew error circle down to a limiting magnitude of about 16 were searched, yielding an average of 3–5 observed possible counterparts per Slew

[8] This was not a dedicated program for stellar identifications, but rather was put into R. R.'s existing program of finding optical counterparts for *HEAO 1* A3 sources (Remillard et al. 1994).

TABLE 3

OBSERVING DETAILS

Observers	Observatory	Telescope and Instrument	Dates	Wavelength Ranges (Å)	Two-Pixel Resolution (Å)
R. R.	MDMO	1.3 m, Mark 3	Since 1991 Jun	3811–5095	4.2
				4500–7103	9.9
S. H. S.....	NSO	McMath-Pierce	Since 1992 Feb	6163–6182	0.05
FBS	ESO	1.5 m, B&C	1992 Dec	3600–7400	3.8
		CAT/CES	1992 Dec	6680–6730	0.1
J. S.....	MMTO	MMT, red channel	1992 Nov, 1993 Apr	3500–7325	6.4
	CTIO	1.5 m, Cass. Spec.	1993 Jan, Aug	3072–7836	16.5
				3570–4518	3.3

NOTE.—R. R.: R. Remillard. S. H. S.: S. Saar. FBS: F. Favata, S. Sciortino, and M. Barbera. J. S.: J. Schachter.

© American Astronomical Society • Provided by the NASA Astrophysics Data System

1996ApJ...463..747S

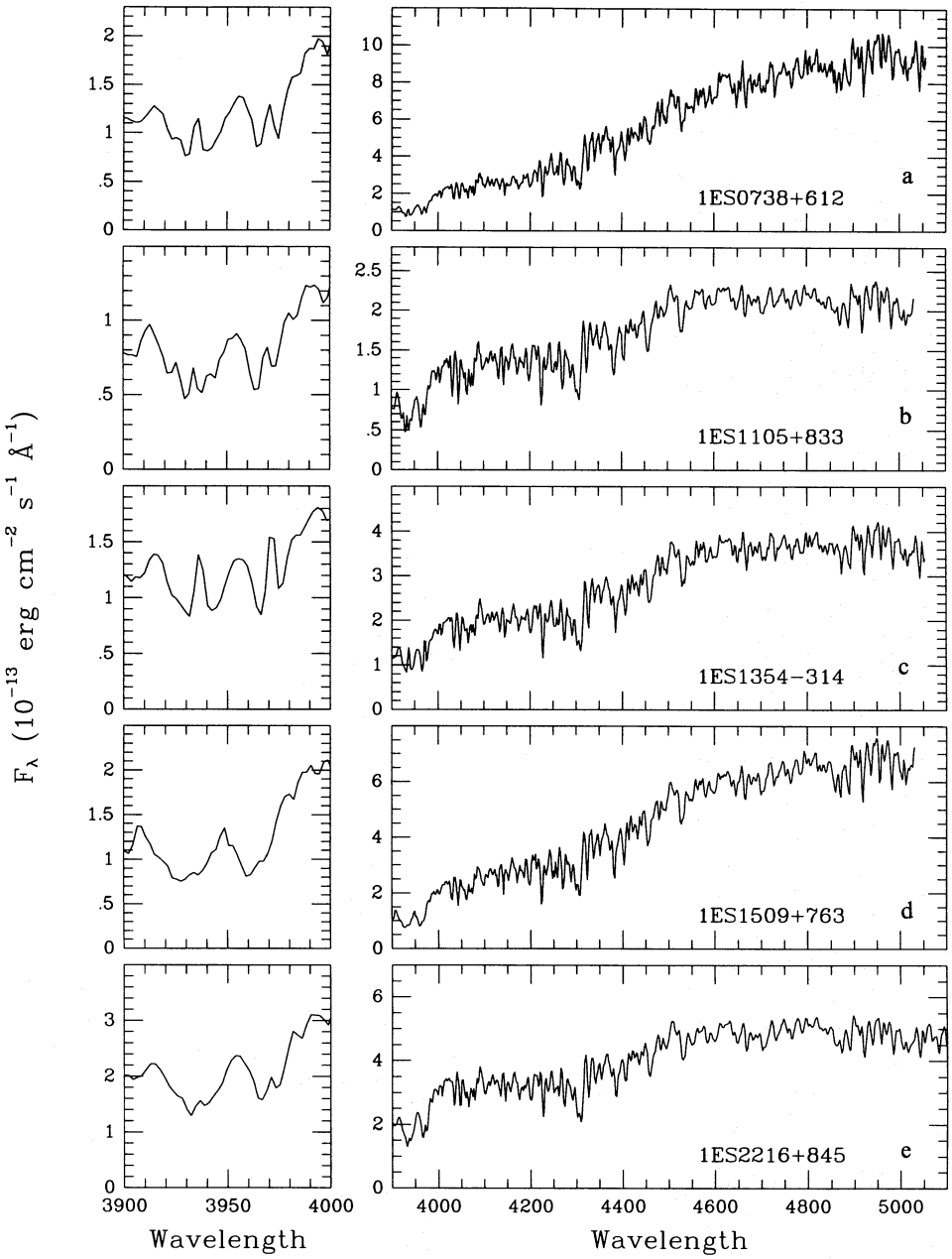

FIG. 3.—Northern observations. Examples of confirmations of stellar activity by low-resolution (R. R.; *a*, *b*, *c*, *d*, *e*) and echelle (S. H. S.; *f*, *g*, *h*) spectroscopy. See Tables 1 and 3 for more details on observers and observational methods. (*a*) 1ES 0738+612 = HD 61396 (K0): evident Ca H and K emission. (*b*) 1ES 1105+833 = SAO 18249 (K2): weaker, but distinguishable, Ca H and K emission. (*c*) 1ES 1354−314 = HD 121688 (K0 V), clearly showing strong Ca H and K emission [also see (*h*)]. (*d*) 1ES 1509+783 = HD 135363 (G5): weak amount of activity, as indicated by squared-off absorption troughs. (*e*) 1ES 2216+845 = SAO 3717 (K2): weak Ca emission features. (*f*) 1ES 1327−313 = HD 117310 (K1 III). This source has a rather low rotation velocity (5 km s^{-1}), determined with a simple line transfer model as in § 2 but shows filled-in Ca H and K. However, a portion of the supercluster of galaxies Shapley 8, a known X-ray source (Breen et al. 1994), falls within the Slew error circle. We speculate that HD 117310 is only a minor contributor, if at all, to the X-ray flux. (*g*) 1ES 1354−314 = HD 121688 (K0 V). A fast rotator. The slowly rotating K1 star HD 155885 was convolved with a rotational broadening function (e.g., Gray 1988) to match the target star. (*h*) 1ES 1614+446 = HD 146696 (G0). Initial low-resolution spectroscopy suggested that this source might be active. This is confirmed by our echelle work. In our analysis the F9 dwarf 10 Tauri was broadened [as in (*g*)] to match the spectrum.

source. In some cases, the glare of nearby bright stars made this difficult. For the bright ($V < 11$), spectral type F–K stars, we used the CAT/CES to measure Li I 6706 Å equivalent widths and rotational velocities. These measurements are described in Favata et al. (1995). See Table 1 (notation "FBS") for details of the observations.

Of the southern fields with multiple possible, or ambiguous, identifications, three were observed with *ROSAT* HRI (AO4) snapshot observations, and six more have recently been observed (the last in 1995 April) in *ROSAT* AO5.

The southern $v \sin i$ measurements nicely complement the northern ones. Given the lower spectral resolution of the ESO CAT observations compared with those from McMath-Pierce (Table 3), the ESO observations accent $v \sin i$ measurements of earlier type coronal stars (F and G), whereas the McMath-Pierce observations are more suited to G and K stars.

In a few notable cases (see notes to tables), the proposed counterparts based on our catalog searches (usually the brightest star in the error circle) turn out *not* to be the most

© American Astronomical Society • Provided by the NASA Astrophysics Data System

1996ApJ...463..747S

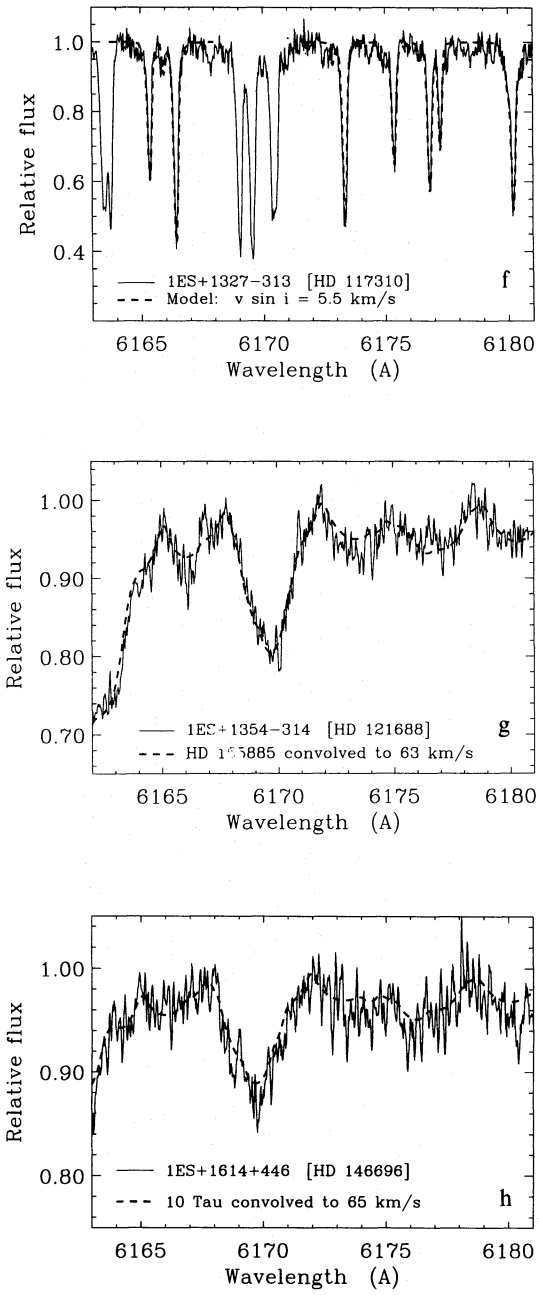

Fig. 3.—*Continued*

likely identification; or, some fainter object in the error circle is much more active. In particular, faint dMe stars in the error circle can explain at least part of the X-ray flux for two of the proposed yellow giants. These results stress the importance of observing all the plausible objects in any given error circle, not just the brightest one.

2.4. *Radio Observations: New Slew RS CVn Systems*

It has been suggested that radio observations of unidentified X-ray sources are a good way of finding new RS CVn systems (Drake, Simon, & Linsky 1992, hereafter DSL92; Drake 1993). Indeed, DSL92 specifically searched for Slew RS CVn systems, starting from a private list of RS CVn candidates, and performing new VLA observations. Of their sources, only one in part A of Table 1 (1ES 0120+004) was not previously known to be active. Radio data from Becker, White, & Edwards (1991) shows that the source 1ES 0738+612 is associated with a 6 cm source of flux 29 mJy. Hence, it may also be an RS CVn system.

Some 15 other stars in Table 1 can probably be ruled out as RS CVn stars, due to their nondetections in VLA or Australia Telescope data in observations performed as filler in our BL Lac identification program (Schachter et al. 1993). These VLA sources have $f_{6\,\mathrm{cm}} < 0.5$ mJy: 1ES 0013+195, 1ES 0238+057, 1ES 0305−284, 1ES 0424+099, 1ES 0437−046, 1ES 1456−400, 1ES 2149+054, and 1ES 2326+411. These Australia Telescope sources have $f_{6\,\mathrm{cm}} < 2$ mJy: 1ES 0154−518, 1ES 0226−615, 1ES 0625−600, 1ES 1002−559, 1ES 1126−610, 1ES 1902−524, and 1ES 2152−548.

2.5. *Other Notable New X-Ray Stars*

Especially notable of the new X-ray sources is an A star candidate, 1ES 1126−610, although this may be a binary star with a cool star companion. Our upcoming *ROSAT* HRI snapshot observations (§ 2.3.2) of this source may help to clarify this issue. There are two cooler (G and K) stars with unusually high $v \sin i$-values (see Fig. 3): 1ES 1354−314 (=HD 121688) and 1ES 1614+446 (=HD 146696). Both appear to be single and the former is listed as a dwarf, which, combined with the high $v \sin i$-values, suggests extreme youth. We recommend further spectroscopic observations to check for companions and the presence of Li I, and to determine the luminosity classes of these two objects.

We find that the previously known chromospherically active Hyades stars 1ES 0415+231 (=HD 284303) and 1ES 0429+130 (=HD 286839) are X-ray sources. Other than the binary cases specifically mentioned in Table 1, we note that 1ES 0603−484 and 1ES 0637−614 are close binaries (Corbally 1984).

In the process of confirming stellar activity in these stars, four unexpected, unusual stellar X-ray optical counterparts have been identified with Slew sources. There are two new T Tauri stars—1ES 0638+094 and 1ES 0625−600 (see below)—and two new cataclysmic variables: 1ES 0437−046 (=BF Eri) and 1ES 1536+516.

We make note of our observations of three groups of active stars not discussed in the main text. In Table 4, we present active stars discovered by one of us (J. S.) in optically blank fields—that is, Slew Survey fields where there was no cataloged stellar counterpart, and no obvious optical counterpart seen on an inspection of the sky survey plates. Note that this approach is different than the approach described above, namely, confirming previously proposed identifications and searching for activity therein. One is 1ES 0625−600. We expect that the others, given the optical magnitudes, estimated from the sky survey plates, are M dwarves.

Table 5 contains new observations of stars previously reported to be X-ray emitters in the literature, but with no optical confirmation of their activity or erroneously determined optical counterparts. Table 6 contains stars not found in the list of 819 sources presented in Elvis et al. (1992). These sources were rejected because they had small numbers of detected photons and their false-source rate was systematically higher than the rest of the survey (see Fig. 12 of Elvis et al. 1992). We note that two stars incorrectly included in Table 7 of Elvis et al. due to typographical errors fall into this same category: 1ES 0923−530 (=SAO 236956, F7 V) and 1ES 1348−588 (SAO 241229, B9 IV).

© American Astronomical Society • Provided by the NASA Astrophysics Data System

1996ApJ...463..747S

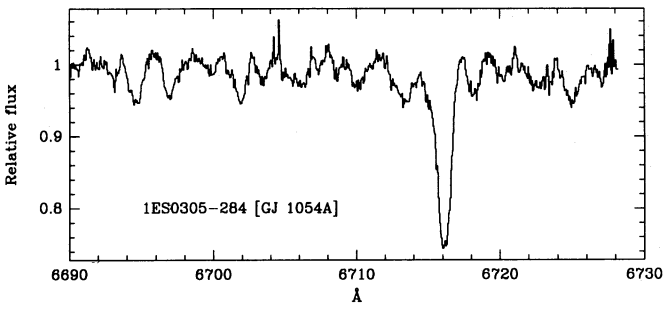

FIG. 4*a*

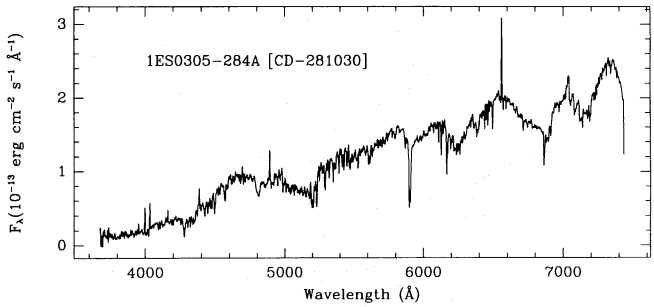

FIG. 4*b*

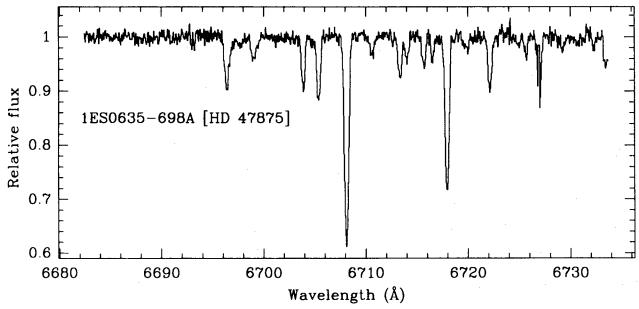

FIG. 4*c*

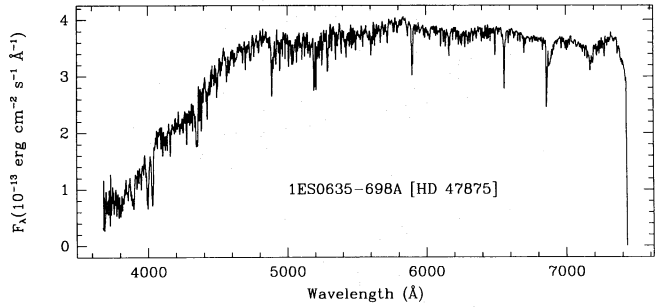

FIG. 4*d*

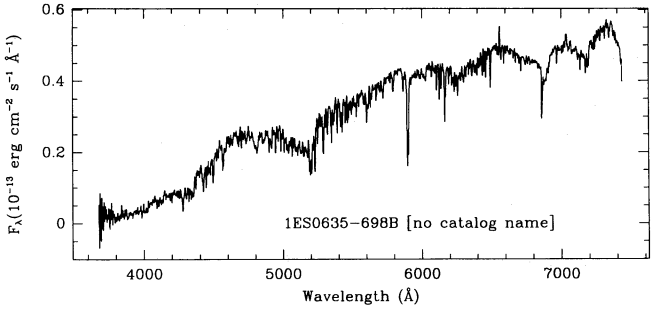

FIG. 4*e*

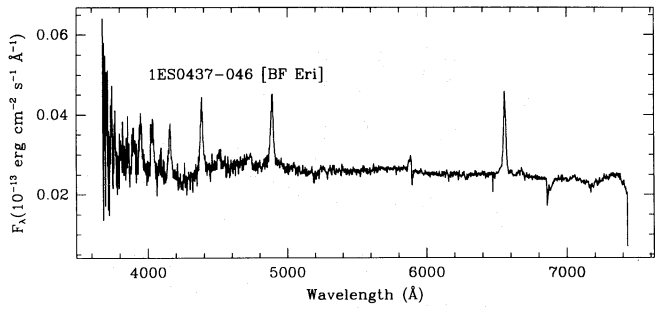

FIG. 4*f*

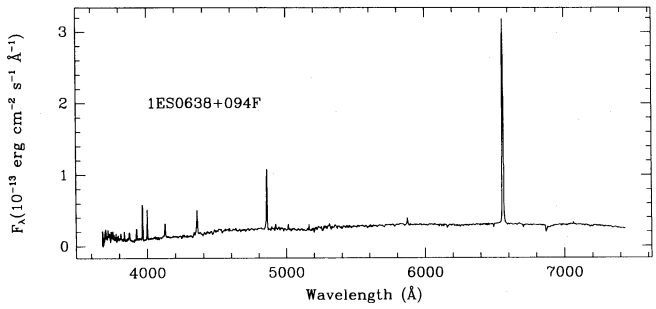

FIG. 4*g*

FIG. 4.—Southern observations. Examples of confirmations of stellar activity by high- and low-resolution spectroscopy (F. F., S. S., and M. B.). See Tables 1 and 3 for more details on observers and observational methods. (*a*, *b*) 1ES 0305−284 = GJ1054A (K7 V). A fast rotator showing strong Li I absorption (*a*), clearly showing Ca H and K emission and Balmer series lines (*b*). (*c*, *d*, *e*) 1ES 0635−698 (Two active stars, HD 47875 denoted as "A" and the uncataloged star as "B"; see notes to Table 1): Star "A" is a relatively fast rotator [10 km s^{-1}; (*a*)]. The Ca H and K lines are filled in for star B. (*f*) 1ES 0437−046. A new CV discovered in our optical identifications work. The cataloged (SIMBAD) star was a variable star of unknown type. (*g*) 1ES 0638+094. One of two new T Tauri stars discovered in our identifications work. This star was found in our observations of the Monoceros region.

3. DISCUSSION

Most of the sources in part A of Table 1 are cool (spectral type later than F), unevolved stars, i.e., stars where coronal activity from magnetic heating is producing the X-ray emission. The sources in part A of Table 1 with $13 < V < 19$, which are the strongest X-ray emitters of all the new X-ray sources, are few in number: 1ES 0013+195, 1ES 0437−046, 1ES 1841−044, and 1ES 2326+411. We have already noted 1ES 0437−046 as a new cataclysmic variable. The log f_X/f_V-values of 1ES 0013+195, and 1ES 2326+411 are typical of very active dMe flare stars, while 1ES 1841−044 has a log f_X/f_V-value (0.72) too extreme for a normal coronal stellar source, suggesting a different origin of the X-ray emission. None of the $13 < V < 19$ sources are bright enough to have been studied in previous surveys for chromospheric emission.

3.1. *Single Stars: v* sin *i and Radius Correlations with* L_X

We can gain insight into the X-ray production mechanisms in active stars by studying the correlation of X-ray luminosity with physical properties of the stars. We use all Slew Survey stars (new ones from part A of Table 1; others

© American Astronomical Society • Provided by the NASA Astrophysics Data System

1996ApJ...463..747S

TABLE 4

ACTIVE STARS DISCOVERED IN OPTICALLY BLANK FIELDS

1ES Name	Estimated V	Other X-Ray Detections	Activity Indicators
1ES 0424+099.....	16.5:	...	dist. HK
1ES 0625−600.....	...	RASS	T Tauri
1ES 2025+573.....	16.0:	...	dist. HK
1ES 2149+054.....	12.0:	RASS	dMe
1ES 2152−548.....	14.3:	RASS, *ROSAT* WFC	HK emission

TABLE 5

NEW INFORMATION ON PREVIOUSLY REPORTED X-RAY STARS

1ES Name	Optical Name	Type	Previous X-Ray	New Optical Info
1ES 0004+287.....	HD 166	K0	EMSS	R. R., SS: 6 km s^{-1}
1ES 0238−009.....	HD 16765	F7 IV	*EXOSAT*	FBS: 31 km s^{-1}
1ES 0250−129.....	HD 17925	K1 V	IPC	S. H. S.: 3.5 km s^{-1}
1ES 0327−242.....	HD 21703	K4 V	EMSS	FBS: $<$ 8 km s^{-1}
1ES 0413−625.....	HD 27256	G8 II–III	EMSS,IPC	FBS
1ES 0457+017.....	HD 26923	G0 IV	IPC	FBS: 14 km s^{-1}
1ES 0510−162.....	HD 33904	B9 IV	IPC, *EXOSAT*	FBS
1ES 0524−711.....	BI 156	dMe	IPC	FBS
1ES 0528−654.....	HD 36705	K1 IIIp	IPC,*EXOSAT*	FBS
1ES 0638+094.....	MON. STARS	...	IPC, *EXOSAT*	FBS: T Tauri
1ES 2201+826.....	HD 209943	F5	*EXOSAT*, WFC	R. R.

NOTE.—1ES 0238−009: Known binary (Pannunzio & Morbidelli 1984). Fast rotator with strong Li I absorption visible. 1ES 0250−129: Unusually strong Li (Cayrel de Strobel & Cayrel 1989). 1ES 0413−625: A G8 III object (m_V = 3.35), it shows weak Li I absorption, compatible with its being an active giant. It also has a faint (~12 mag) companion for which we have observed a late dKe type. Most likely a composite X-ray source, as both counterparts are likely emitters. 1ES 0510−162: A bright (m_V = 3.3) B9 star, with a faint (m_V ~ 13) dMe companion. B9 appears to have a completely normal spectrum, so that X-ray flux is most likely entirely due to the companion. 1ES 0524−711: Classified as Be in Brunet et al. 1975. We observe a normal G type star (definitely not a B) with a dMe companion. We consider X-ray flux as most likely due to the dMe companion, also given its extreme Hα emission. 1ES 0528−654: A well-known active PMS star (AB Dor), it has a dMe companion within 1′; both are likely to be X-ray sources. 1ES 0638+094: Slew field contains part of the Monoceros region. There is a bright (m_V = 4.46) O7 Ve counterpart near the Slew position. We have also found a T Tauri in the error circle. X-ray source likely to be composite. 1ES 2201+826: Ambiguity removed (HD 209942 also in error box; Elvis et al. 1992).

TABLE 6

ACTIVE STARS NOT IN SLEW CATALOG

1ES Name	Optical Name	Type	Optical Info
1ES 0133+484.....	HD 9746	K1 III	St90
1ES 0308−055.....	HD 19754	K0	RS CVn (DSL89)
1ES 0428+366.....	HD 28591	K III+	Binary, St90
1ES 1753+362.....	HD 163621	G5	R. R., S. H. S.: 10 km s^{-1}, RS CVn (DSL89)
1ES 1811+006.....	HD 167108	G8 IV	R. R.
1ES 1928+233.....	HD 344462	F5	R. R.: Ca II, Hβ
1ES 2005+160.....	HD 191179	G5	S. H. S.: SB2, 12 km s^{-1}

NOTES.—DSL92: RS CVns (Drake et al. 1989). St90: Strassmeier et al. 1990. Other references are as in Table 1.

from Elvis et al. 1992) that have rotational velocities either from our observations, from SIMBAD, or other references in the literature (Table 7). The analogous sample of binary stars (Table 8) is discussed later.

Binaries were specifically noted in part A of Table 1 and in the text (§§ 2.4 and 2.5). Twenty of the 39 single stars have known parallaxes.

For the remaining 19 (1ES 0004+287, 1ES 0157+706, 1ES 0226−615, 1ES 0238+057, 1ES 0305−284, 1ES 0357−400, 1ES 0418+281, 1ES 0459−753, 1ES 0528−654, 1ES 0740+228, 1ES 1328+244, 1ES 1354−314, 1ES 1435−606, 1ES 1614+446, 1ES 1704+545, 1ES 1716+551, 1ES 1824+151, 1ES 1833+169, 1ES 2153+441) we derived physical distances from distance moduli, using the following assumptions:

1. Adopt B-magnitudes, V-magnitudes, and spectral types from SIMBAD.
2. Use intrinsic (i.e., unreddened) $B-V$-values from Mihalas & Binney (1981, and references therein), and values of M_V and $R/R_\odot$ values from Allen (1975), interpolating over luminosity classes and over spectral types when necessary.
3. Assume all stars without known classes (of which there are 7) are dwarfs. All but one of these are type K0 or later.

© American Astronomical Society • Provided by the NASA Astrophysics Data System

1996ApJ...463..747S

TABLE 7

SINGLE STAR ROTATION VELOCITIES, LUMINOSITIES, AND RADII

Index (1)	1ES Name (2)	Other Name (3)	Spectral Type (4)	$v \sin i$ (km s^{-1}) (5)	log R (km) (6)	log ($\Omega \sin i$) (rad s^{-1}) (7)	log L_X (ergs s^{-1}) (8)
			A: F7–M5 Stars				
1.....	1ES 0004+287	HD 166	K0 V	6.0 [S. H. S.]	5.78	−5.00	28.60
2.....	1ES 0041−182	β Cet/4128	K0 III	<5 [E90]	7.05	<−6.35	29.66
3.....	1ES 0238+057	BD +05 378	M1	<8 [FBS]	5.63	<−4.73	29.14
4.....	1ES 0250−129	HD 17925	K1 V	3.9 [S. H. S.]	5.77	−5.18	28.21
5.....	1ES 0305−284	CD-28 1030	K7 V	30.0 [FBS]	5.66	−4.18	29.27
6.....	1ES 0316+031	κ Cet/20630	G5 V	4.5 [SB92]	5.82	−5.17	28.51
7.....	1ES 0357−400	HD 25300	K0	12.0 [FBS]	5.78	−4.71	29.93
8.....	1ES 0418+281	V987 Tau/283572	G2 III	95.0 [W87]	6.73	−4.75	31.95
9.....	1ES 0423+146	π Tau/28100	G7 III	8.0 [Sbd]	6.93	−6.02	29.98
10.....	1ES 0457+017	GJ 182	M1 Ve	14 [FBS]	5.63	−4.47	29.13
11.....	1ES 0459−753	HD 32918	K1 IIIp	45.0 [P90]	7.09	−5.43	32.18
12.....	1ES 0504−575	GJ 189	F8 V	17.0 [S89]	5.89	−4.66	29.30
13.....	1ES 0528−654	AB Dor/36705	K1 IIIp	93.0 [KSC94]	7.09	−5.12	31.59
14.....	1ES 0740+228[a]	BD +23 1799	K0 III/IV	17.0 [S. H. S.]	6.73	−5.50	31.94
15.....	1ES 0742+036	YZ CMi	M4.5 Ve	4.8 [MC92]	5.38	−4.70	28.31
16.....	1ES 0834+651	π^1 UMa/72905	G1.5 Vb	9.0 [G84]	5.85	−4.90	29.10
17.....	1ES 1249+278	31 Com/111812	G0 III	63.0 [E90]	6.65	−4.82	30.84
18.....	1ES 1252−060	BD −05 3596	K5	<8 [FBS]	5.71	<−4.80	29.02
19.....	1ES 1309+281	β Com/114710	F9.5 V	3.9 [G84]	5.87	−5.28	28.20
20.....	1ES 1314+096	59 Vir/115383	G0 Vs	6.9 [S. H. S., L94]	5.87	−5.03	28.91
21.....	1ES 1328+244	FK Com	G5 II	162.5 [H93]	7.41	−5.20	32.92
22.....	1ES 1332−080	EQ Vir/118100	K5 Ve	9.9 [S86]	8.45	−7.45	29.16
23.....	1ES 1354−314	HD 121688	K0 V	63.0 [S. H. S.]	5.78	−3.98	29.72
24.....	1ES 1423+520	GJ 549A	F7 V	29.0 [S89]	5.89	−4.43	29.08
25.....	1ES 1435−606	α Cen AB	G2 V	3.0 [P81]	5.85	−5.37	27.28
26.....	1ES 1547+262	δ CrB/141714	G3.5 III	8.0 [Sbd]	6.79	−5.89	30.30
27.....	1ES 1614+446	HD 146696	G0	65.0 [S. H. S.]	5.87	−4.05	30.05
28.....	1ES 1716+551	SAO 030326	K0	5.0 [S. H. S.]	5.78	−5.08	28.50
29.....	1ES 1810+696	HD 167605	K2 V	<10 [F89]	5.76	<−4.75	28.97
30.....	1ES 1824+151	HD 170052	K0 V	17.0 [S. H. S.]	5.78	−4.55	29.79
31.....	1ES 1833+169	HD 171746	G2 V+G2 V	5.0 [S. H. S.]	5.85	−5.15	29.13
32.....	1ES 1902−524	ρ Tel/177171	F7 V	46.0 [Sbd]	5.89	−4.23	30.86
33.....	1ES 1932+695	σ Dra/185144	K0 V	1.5: [G84][b]	5.78	−5.60	27.72
34.....	1ES 2153+441	HD 208472	K0	18.0 [S. H. S.]	5.78	−4.52	28.95
			B: Early F Stars				
35.....	1ES 0157+706	NSV 694	F2 V	10.0 [S. H. S.]	5.96	−4.96	29.84
36.....	1ES 0226−615	HD 15638	F3 IV/V	62.0 [FBS]	6.17	−4.37	31.20
37.....	1ES 1246+605	HD 111456	F5 V	37.0 [Sbd]	5.91	−4.34	29.25
38.....	1ES 1704+545	μ Dra	F5	20.0 [F89]	5.91	−4.61	28.71
39.....	1ES 1935+501	13 Cyg/185395	F4 V	7.0 [Sbd]	5.92	−5.07	28.76

NOTE.—In col. (3), numbers following the slash ("/") refer to the HD catalog. 1ES 0412+060 was eliminated because there is a known RS CVn in the Slew field, making the calculation of L_X difficult. AD Leo (=1ES 1016+201) was eliminated because its 2.7 day period implies a rather pole-on configuration. References for $v \sin i$ measurements are as follows. E90: Eaton 1990. F89: Fleming et al. 1989. FBS: Favata, Barbera, and Sciortino in this paper. G84: Gray 1984. H93: Huenemoerder et al. 1993. KSC94: Kuerster et al. 1994. L94: Linsky et al. 1994. MC92: Marcy & Chen 1992. P81: Pallavicini et al. 1981. P90: Piskunov et al. 1990. Sbd: SIMBAD stellar database, and references therein. SB92: Saar & Baliunas 1992. S. H. S.: S. Saar in this paper. S86: Saar et al. 1986. S89: Soderblom et al. 1989. W87: Walter et al. 1987.

[a] S. H. S. "by eye" estimate of spectral type looks like K0 III/IV, although SIMBAD lists type as K0.

[b] This star is rather inactive, and may be present in the Slew primarily because of its proximity to the Sun. It does, however, have Ca H and K emission, with levels varying over 6–7 yr timescales (Gray et al. 1992).

The firm evidence that X-ray emission drops for giants later than K1–2 as deduced from the *Einstein* survey of giants and supergiants (Maggio et al. 1990), recently confirmed by the *ROSAT* All-Sky Survey (Haisch, Schmitt, & Rosso 1991) indicates that these are most likely to be dwarfs.[9] We classify 1ES 0238+057 (BD+05 378; spectral type M in SIMBAD) as an M1, based on our ESO B&C spectra.

As a check, we applied our distance determination approach to the stars in Table 7 with known parallaxes, finding it to be completely consistent with that approach. We excluded apparently single stars that might be binaries viewed pole-on, using the criteria of Fleming et al. (1989, hereafter F89; $L_X > 10^{30.5}$ and $v \sin i < 10$ km s^{-1}). Analogously, we excluded AD Leo (=1ES 1016+201) because of its low inclination, and HD 117310 (=1ES 1327−313) because of its proximity to the Shapley 8 supercluster (see Fig. 3).

We scaled our IPC count rates down by a factor of 1.19 (see § 5 of Elvis et al. 1992) to convert the fluxes to the more usual 0.3–3.5 keV range (e.g., F89). Assuming a Raymond-Smith log $T = 6.6$ model and column density $N_H = 10^{20}$ cm^{-2}, we find a conversion factor of (1.4/1.19)

[9] We have checked that, under the assumption that these stars are subgiants instead of dwarfs, the correlation results presented below are unchanged.

© American Astronomical Society • Provided by the NASA Astrophysics Data System

1996ApJ...463..747S

TABLE 8

BINARY STAR ROTATION VELOCITIES, LUMINOSITIES, AND RADII

Index (1)	1ES Name (2)	Other Name (3)	Spectral Type (4)	$v \sin i$ (km s^{-1}) (5)	log R (km) (6)	log ($\Omega \sin i$) (rad s^{-1}) (7)	log L_X (ergs s^{-1}) (8)
1.....	1ES 0044+239	ζ And	K1 III	40.0 [Ra94]	7.09	−5.49	29.97
2.....	1ES 0051−749	CF Tuc/5303	K4 IV	35.0 [St93]	6.47	−4.92	30.09
3.....	1ES 0054+231	η And/5516	G8 III	8.0 [BP73]	6.95	−6.04	31.86
4.....	1ES 0114+065	UV Psc/7700	G5 V	66.0 [St93]	5.82	−4.00	30.75
5.....	1ES 0114−027	AY Cet/7672	G5 III	4.0 [St93]	6.85	−6.25	31.08
6.....	1ES 0120+004	BI Cet/8358	G5 V:+G5 V:	60.0 [St93]	5.88	−4.10	29.81
7.....	1ES 0143−253	ϵ Scl/10830	F2 IV	86.0 [BSC]	6.39	−4.45	29.75
8.....	1ES 0150+293	α Tri/11443	F6 IV	100.0 [Ba90]	6.20	−4.20	29.27
9.....	1ES 0209+300	BD +29 371	G5 III+	16.0 [UF70]	6.85	−5.64	32.22
10.....	1ES 0232−440	CC Eri/16157	K7 Ve	15.0 [St93]	5.83	−4.65	29.48
11.....	1ES 0238−009	HD 16765	F7 IV	31.20 [FBS]	6.22	−4.72	29.81
12.....	1ES 0241−381	UX For/17084	G6.5 V	50.0 [St93]	5.81	−4.11	30.56
13.....	1ES 0245+309	VY Ari/17433	K3.5 IV/V	6.0 [St93]	6.10	−5.32	29.78
14.....	1ES 0323+285	UX Ari/21242	K0 IV	37.0 [St93]	6.41	−4.84	31.10
15.....	1ES 0327−242	HD 21703	K4 V	14.0 [Fa95]	5.70	−4.55	29.09
16.....	1ES 0334+004	V711 Tau/22468	K1 IV	13.0 [St93]	6.43	−5.31	30.88
17.....	1ES 0407−080	EI Eri/26337	G5 IV	50.0 [St93]	7.40	−5.70	31.21
18.....	1ES 0419+149	BD +14 690/27691	G0 V	8.0 [St93]	5.87	−4.96	29.19
19.....	1ES 0423+154	V777 Tau/28052	F0 V	193.0 [BP73]	5.98	−3.69	31.61
20.....	1ES 0433+270	V833 Tau/283750	dK5e	6.30 [St93]	5.72	−4.92	29.46
21.....	1ES 0441−107	RZ Eri/30050	K0 IV	11.0 [St93]	6.48	−5.44	30.56
22.....	1ES 0447+068	HD 30652	F6 V	10.0 [Pa92]	5.91	−4.91	28.84
23.....	1ES 0501+589	12 Cam/32357	K0 III	12.0 [Ra94]	7.05	−5.97	31.08
24.....	1ES 0538+037	V1149 Ori/37824	K1 III	11.0 [St93]	7.09	−6.05	29.52
25.....	1ES 0637−614	HD 48189	G1.5 V	15.0 [Je95]	5.85	−4.68	29.48
26.....	1ES 0731+319	YY Gem	dM1e	40.0 [St93]	5.60	−4.00	29.39
27.....	1ES 0736+053	HD 61421	F5 IV	4.5 [Be84]	6.19	−5.53	28.42
28.....	1ES 0740+290	σ Gem/62044	K1 III	28.0 [Ra94]	7.09	−5.64	31.02
29.....	1ES 0758+574	54 Cam/65626	G5 IV	14.0 [Ra94]	6.34	−5.19	29.73
30.....	1ES 0836+319	RZ Cnc/73343	K1 III	25.0 [St93]	7.10	−5.70	31.50
31.....	1ES 0919+404	BF Lyn/80715	K2 V	10.0 [St93]	5.76	−4.75	30.01
32.....	1ES 0930+700	HD 82210	G4 III/IV	4.90 [G85]	6.57	−5.88	29.89
33.....	1ES 0957+247	DH Leo/86590	K0 V	45.0 [St93]	5.78	−4.12	30.16
34.....	1ES 1002−559	HD 87525	K1.5 III	16.0 [St93]	7.11	−5.90	31.71
35.....	1ES 1052+607	DM UMa	K0.5 II/IV	27.0 [St93]	7.07	−5.64	31.15
36.....	1ES 1115+318	ξ UMa B/98230	G5 V	2.80 [St93]	5.82	−5.37	29.37
37.....	1ES 1137−651	HD 101379	K2–4	<10.0 [St93]	5.75	<−4.75	31.57
38.....	1ES 1138+522	RW UMa	K0 IV	27.0 [St93]	6.48	−5.05	30.75
39.....	1ES 1145+204	93 Leo/102509	G5 IV	5.0 [St93]	7.40	−6.70	29.89
40.....	1ES 1213+728	DK Dra/106677	K1 III	10.0 [St93]	7.10	−6.10	31.16
41.....	1ES 1239−011	HD 110379	F0 V	25.0 [UF70]	6.0	−4.58	29.15
42.....	1ES 1259+289	UX Com	K1 IV	15.0 [St93]	5.9	−4.67	31.34
43.....	1ES 1308+361	RS CVn/114519	G9 IV	42.0 [St93]	6.4	−4.77	31.26
44.....	1ES 1332+374	BH CVn/118216	F2 IV	12.0 [Ra94]	6.39	−5.31	30.70
45.....	1ES 1340−611	V851 Cen/119285	K2 III/IV	6.5 [St93]	5.85	−5.04	30.81
46.....	1ES 1449+193	ξ Boo/131156	G8 V	2.7 [G84]	5.80	−5.36	28.73
47.....	1ES 1502+478	HD 133640	G0 V	15.0 [BP73]	5.87	−4.69	29.67
48.....	1ES 1556+257	MS Ser/143313	K2 V	16.0 [OS96]	5.76	−4.55	29.37
49.....	1ES 1612+339	σ^2 CrB/146361	G0 V	25.0 [St93]	5.87	−4.47	30.15
50.....	1ES 1638+608	WW Dra/150708	K0 IV	43.0 [St93]	6.48	−4.84	31.22
51.....	1ES 1734+742	29 Dra/160538	K0–2	8.0 [St93]	5.77	−4.87	30.96
52.....	1ES 1802+025	HD 165341A	K0 V	<5.0 [S. H. S.]	5.78	<−5.08	27.98
53.....	1ES 1832+516	BY Dra/234677	K4 V	8.0 [St93]	5.73	−4.83	29.55
54.....	1ES 1907+523	V1762 Cyg/179094	K1 III/IV	15.0 [St93]	6.76	−5.58	31.87
55.....	1ES 2013+448	HD 192785	K0	12.0 [S. H. S.]	5.78	−4.70	28.73
56.....	1ES 2038−007	HD 197010	F8	100.0 [F89]	5.89	−3.89	29.86
57.....	1ES 2052+441	V1794 Cyg/199178	G2 V	80.0 [H86]	5.85	−3.94	30.0
58.....	1ES 2058+398	V1396 Cyg	M2 V	4.3 [St93]	5.55	−4.92	29.17
59.....	1ES 2100+276	ER Vul/200391	G5 V	85.0 [St93]	5.82	−3.89	30.23
60.....	1ES 2159+436	RT Lac/209318	G9 IV	49.0 [St93]	6.40	−4.71	30.86
61.....	1ES 2202+469	HK Lac/209813	K0 II	15.0 [St93]	7.85	−6.67	30.99
61.....	1ES 2206+455	AR Lac/210334	K0 IV	81.0 [St93]	6.48	−4.57	30.77
62.....	1ES 2236−208	FK Aqr/214479	dM2e	7.0 [St93]	5.55	−4.70	30.82
63.....	1ES 2257−340	TZ PsA/217344	G5 VP	71.9 [FBS]	5.82	−3.96	29.81
64.....	1ES 2307+476	KZ And/218738	dK2	11.6 [St93]	5.76	−4.69	29.59
65.....	1ES 2335+461	λ And/222107	G8 III/IV	6.5 [D95]	6.67	−5.85	30.33
66.....	1ES 2352+283	II Peg/224085	K2.5 IV/V	21.0 [St93]	6.10	−4.77	29.09

NOTE.—Variable star names and HD numbers given when available; otherwise accepted name or names from SIMBAD. Rotational velocity references are as follows. BP73: Bernacca & Perinotto 1973. BSC: Hoffleit & Jaschek 1982. Ba90: Balachandran 1990. Be84: Benz & Mayor 1984. D95: Donati et al. 1995. FBS: Favata, Barbera, and Sciortino in this paper. Fa95: Favata et al. 1995. G84: Gray 1984. G85: Gray & Nagar 1985. H86: Huenemoerder 1986. Je95: Jeffries 1995. OS96: Osten & Saar 1996. Pa92: Pan et al. 1992. Ra94: Randich 1994. S. H. S.: S. Saar in this paper. St93: Strassmeier et al. 1993. UF70: Uesugi & Fukuda 1970.

© American Astronomical Society • Provided by the NASA Astrophysics Data System

1996ApJ...463..747S

$\times 10^{-11} = 1.2 \times 10^{-11}$ ergs cm^{-2} (IPC count)$^{-1}$. The choice of N_H is a reflection of the nearness of the X-ray selected coronal star population. Note that F89 used a conversion factor of 2.0×10^{-11} ergs cm^{-2} (IPC count)$^{-1}$, corresponding to higher temperatures (log $T \geq 6.8$) for any reasonable N_H. We normalize their values of flux to our convention for the discussion below.

In part A of Table 7 we list the derived values of $v \sin i$, stellar radius R, X-ray luminosity, and angular velocity for the F7–M5 stars, the same selection criteria that F89 and Pallavicini et al. (1981, 1982) used, to ease comparison with those samples. The remaining early F stars are listed in part B of Table 7.

We tested for correlations between L_X and the other quantities using the nonparametric Spearman rank-order coefficient and the even more nonparametric Kendall's τ (details in Press et al. 1986). We prefer Kendall's τ, which is known to be more reliable for a small number of data points (<30) when both detections and upper limits are included. In fact, in all cases the two approaches gave identical qualitative results. The upper limits provide important information for the correlations and can be included by using the ASURV survival analysis package (version 1.1). In our sample, three F7–M5 stars have upper limits, while in the F89 sample more than half the stars do (38 of 54 in the published F89 sample; but see below).

For the sources in part A of Table 7, we find that both $v \sin i$ and R correlate with L_X at the 99.9% level (Tables 9A–9D). That is, we can reject the null hypothesis of no correlation at this level. We find, however, that $\Omega \sin i$ is formally uncorrelated with L_X.

To compare these results with F89, we reanalyzed their

TABLE 9A

SINGLE STARS: CORRELATION TESTS

	SLEW		EMSS		COMBINED	
PARAMETER	Kendall's τ	Confidence Level	Kendall's τ	Confidence Level	Kendall's τ	Confidence Level
$v \sin i$.....	5.99	99.9%	1.90	94.2% (90.9%)	5.11	99.9%
$\Omega \sin i$.....	0.94	65.2% (34.5%)	0.63	46.8% (75.9%)	0.05	4.2% (37.6%)
Radius.....	3.41	99.9%	4.61	99.9%	4.68	99.9%

NOTE.—Slew Survey single star sample from part A of Table 7; F89 single stars from their Table 1 (no possible pole-on binaries or pre–main-sequence stars; spectral types F7–M5 only). Slew Survey binary star sample from Table 8; F89 binary sample composed of sources in their Table 2 that have given values of $v \sin i$, both upper limits and detections. In correlations, confidence level is for rejecting the null hypothesis that the given parameter is uncorrelated with L_X. Whenever there are significant differences between the Kendall's τ and rank-order confidences, we report the rank-order confidence in parentheses, for comparison. Upper limits to $v \sin i$ are excluded from the regression analyses.

TABLE 9B

BINARY STARS: CORRELATION TESTS

	SLEW		EMSS		COMBINED	
PARAMETER	Kendall's τ	Confidence Level	Kendall's τ	Confidence Level	Kendall's τ	Confidence Level
$v \sin i$.....	1.85	93.5%	1.27	79.6%	2.01	95.5%
$\Omega \sin i$.....	1.94	94.8%	0.30	23.9% (40.3%)	2.02	95.6%
Radius.....	4.14	99.9%	1.73	91.6%	5.41	99.9%

TABLE 9C

SINGLE STARS: $v \sin i$ ON L_X LINEAR REGRESSION

	SLEW			COMBINED		
MERIT FUNCTION	Value/d.o.f.	Slope	L_0	Value/d.o.f.	Slope	L_0
$\chi^2: \left(\frac{L_i - L}{\sigma_i}\right)^2$	1081/28	2.45 ± 0.03	26.7 ± 0.04	1610/56	2.31 ± 0.03	26.7 ± 0.04
$\left\lvert\frac{L_i - L}{\sigma_i}\right\rvert$	133/28	2.45	26.76	257/56	2.80	26.07

TABLE 9D

BINARY STARS: STELLAR RADIUS ON L_X LINEAR REGRESSION

	SLEW			COMBINED		
MERIT FUNCTION	Value/d.o.f.	Slope	L_0	Value/d.o.f.	Slope	L_0
$\chi^2: \left(\frac{L_i - L}{\sigma_i}\right)^2$	5752/63	0.68 ± 0.02	26.3 ± 0.11	6199/90	0.76 ± 0.02	25.8 ± 0.10
$\left\lvert\frac{L_i - L}{\sigma_i}\right\rvert$	980/63	3.33	9.53	718/90	2.17	16.85

© American Astronomical Society • Provided by the NASA Astrophysics Data System

1996ApJ...463..747S

sample. We updated six of their upper limits with our own new v sin i detections (HD 18632, 12 km s^{-1}; HD 22853, 18 km s^{-1}; 1E0443.8−1006, 11 km s^{-1}; and GL 900, 5 km s^{-1}) or more restrictive 8 km s^{-1} upper limits (1E0234.8−0210 and HD 117860). We included the remaining F89 sample upper limits explicitly in ASURV. We find that R is correlated with L_X at the 99.9% level, while v sin i and Ω sin i are uncorrelated (Tables 9A–9D). This is consistent with the results of F89. Thus, the main difference between the two samples is that the underlying correlation in the F89 sample is definitely R-L_X.

We created a *combined sample* from the F89 and Slew F7–M5 stars. Although formally the F89 and Slew samples are drawn from different surveys, they are close cousins (even siblings). Both the EMSS and Slew Survey were performed with the same instrument, at the same epoch. The F89 identification with optical counterparts was performed in a manner similar to ours. The only substantive difference is the limiting sensitivity, which is typically a factor of 10 in X-ray flux. Combining the two samples yields a healthy sized group of coronal stars, spanning a wide range of parameter space. While we make no claim that the combined sample is statistically complete in any sense, it is nevertheless appealing to compare the properties of the Slew, F89, and F89 + Slew samples (as we do below).

The only star in common to the F89 and Slew samples is 1ES 1810+696, an F89 upper limit (part A of Table 7). For the combined sample, the correlation of L_X with Ω sin i is definitively ruled out (4.2%; Tables 9A–9D). The R-L_X and v sin i–L_X correlations are at the greater than 99% level.

3.2. *Single Stars: Correlations of Rossby Number (R_0) with L_X*

Other authors (e.g., Schmitt et al. 1985) have suggested that R_0 is correlated with L_X. Schmitt et al. use the equation

$$R_0 = \frac{\pi^2}{2}\frac{R}{(v \sin i)\tau_{conv}}, \quad (1)$$

where τ_{conv} is the convective turnover time. We took values of τ_{conv} for the main-sequence single, late-type stars from Ruciński & Vandenberg (1986; eq. [1]). Note that the v sin i upper limits translate into R_0 *lower* limits.

A significant fraction (28%) of the single star sample in part A of Table 7 is evolved stars (mainly G and K giants), whose values of τ_{conv} are higher than those of dwarfs.[10] Unfortunately, Ruciński & Vandenberg considered only the range $4.5 > \log g > 3.5$. Their adjustment to the main-sequence value of $\log \tau_{conv}$ for G and K giants is greater than 0.5. We use this to deduce R_0 *upper* limits.

As ASURV is unable to work on data with both upper and lower limits in the independent variable, we checked for an L_X correlation with Rossby Number in three subsamples: (1) R_0 detections only, i.e., dwarfs with detected v sin i's; (2) R_0 detections and upper limits, i.e., case 1 with the evolved stars added; and (3) R_0 detections and lower limits, i.e., case 1 with the dwarfs with v sin i upper limits added. A significant correlation (i.e., more than 99% confidence) between L_X and R_0 was found only in case 3 (the others were case 1 with 97.9%, and case 2 with 94.1%). For subsample 1, a least-squares fit gives $\log L_X = 28.75 + (-0.41 \pm 0.24) \times \log R_0$, with the errors calculated via a bootstrap approach in ASURV. The slope differs from earlier results on optically selected samples of stars observed by *Einstein* (Schmitt et al. 1985; Micela, Sciortino, & Serio 1985a), which found $\log L_X \sim -2 \log R_0$ (F89 did not consider R_0 correlations). Hempelmann et al. (1995) found $\log L_X = 28.07 + (-1.02 \pm 0.12) \times \log R_0$ in a X-ray selected sample of coronal stars from the *ROSAT* all-sky survey. This slope is consistent with our results at the 2 σ level.

From equation (1), we see that $R_0 \propto (v \sin i)^{-1}$, as we empirically find for the F7–M5 dwarves in Table 7 that R_0 and R/τ_{conv} are formally uncorrelated (98%). Thus, $L_X \propto R_0^{-0.4}$ is equivalent to $L_X \propto (v \sin i)^{0.4}$ for our sample. Our smaller value of the L_X-R_0 slope is an indication that the L_X–v sin i relation flattens at high v sin i-values (see below). The optically selected samples, which have $L_X \propto (v \sin i)^2$, are expected to give $L_X \propto R_0^{-2}$ (Schmitt et al. 1985).

3.3. *Correlations in Binary Stars*

We also searched for correlations between the various parameters and L_X among the binary stars in the Slew with known velocities (Table 8). We used distances from Strassmeier et al. (1993) when available, or, if not, the parallaxes. When neither were available, we used the approximate distance method of the previous section. The only clear correlation (i.e., more than 99% probability; Tables 9A–9D) for Slew stars was between R and L_X (including radii for the stars with v sin i upper limits). This statement is true whether or not we restrict ourselves to spectral types F7–M5 (as in the single star analysis above). We note that many of the binaries have known inclinations (e.g., Strassmeier et al. 1993). For small sin i (0.25–0.5), the projected rotational velocity may not be a good measure of the activity. Therefore, we reanalyzed the binary subsamples with $i > 15°$ and $i > 30°$. The number of stars excluded were one and seven, respectively. In neither case are the correlations affected.

We confirmed that in the F89 binary sample (stars in their Table 2 with given v sin i) none of the three parameters (v sin i, Ω sin i, or R) correlate with L_X. However, in the combined Slew and F89 + Slew binary star samples, R correlates with L_X at more than 99% probability confidence. The only star in common between the two samples is 1ES 2038−007.[11] In the cases of an R-L_X correlation in binary stars, the slope is approximately linear (Tables 9A–9D). This statement holds for the total Slew binary sample and also for either of the two cuts in inclination angle.

Comparing the Slew single star and binary star samples (Tables 9A–9D), we see that the main difference is that L_X correlates with both v sin i and R in the single star sample, but L_X correlates only with stellar radius in the binary star sample. The same results hold when comparing the combined single star sample to the combined binary sample.

3.4. *Rotational Saturation*

The R-L_X correlation is probably caused by the X-ray selection, which preferentially picks out the most active

[10] In § 3.1, we provided evidence that the stars of unknown luminosity class in part A of Table 7 are main-sequence stars; with this assumption, the adjusted contribution of evolved stars in part A of Table 7 is only 23%. Both the EMSS single star and binary star samples contained a minority fraction of evolved stars: 8% and 24%, respectively.

[11] The star 1ES 0327−242, although not part of the F89 sample (since it had the selection criterion $\delta > -20°$), appears in the EMSS catalog (Stocke et al. 1991).

© American Astronomical Society • Provided by the NASA Astrophysics Data System

1996ApJ...463..747S

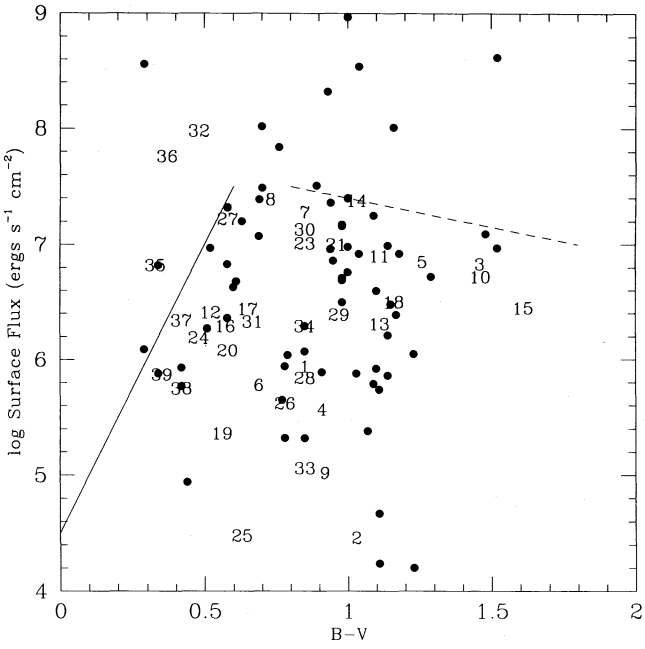

FIG. 5.—Soft X-ray surface flux versus intrinsic $B-V$ color for all Slew survey F0–M5 single stars with v sin i detections or upper limits (*numbers*, corresponding to col. [1] of Table 7), and binaries (*points*, from Table 8), compared with upper bound to F_X from Vilhu & Walter (1987; *solid line*) and to a line of constant $F_X/F_{bol} = 10^{-3}$ (*dashed line*). To enhance readability, seven numeric labels have been displaced slightly from their true positions in the diagram: 10, 23, 38 downward; 3 upward; 31 to the right; 16 to the left; and 39 upward and to the left. The explicit form of the Vilhu & Walter line is $\log F_X = 4.5 + 5(B-V)$. The binary with the anomalously high surface flux at the upper left corner ($B-V = 0.29$, $\log F_X = 8.54$) is 1ES 0423+154 (=HD 28052, SB), an extremely rapidly rotator (v sin $i = 193$ km s^{-1}).

stars. For these stars, the value of L_X depends on the stellar surface area, at a given flux limit. Therefore, we converted the L_X's to surface fluxes (F_X's). Following F89, we plotted F_X as a function of $B-V$ for all the Slew late-type stars with measured v sin i-values (Fig. 3). In the rotational saturation scenario, saturated surface fluxes initially increase with increasing $B-V$ (decreasing values of the stellar mass), from the larger convection zone depths (Vilhu & Walter 1987; F89). However, above $B-V = 0.6$ ($\sim$G0), the saturated flux becomes essentially independent of $B-V$ (e.g., $\sim 7 \times 10^7$ ergs cm^{-2} s^{-1}; F89), presumably because the stellar surface is completely covered. Although our data are more sparse, they are consistent with this picture.

For the reader's convenience, Figure 5 has been plotted in the same scale of the corresponding figure in F89 (their Fig. 6). The main difference between our F_X vs. $B-V$ plot and theirs is that in our case essentially all stars lie below the $F_X/F_{bol} = 10^{-3}$ boundary, where F_{bol} is the bolometric luminosity. Put another way, our figure is more similar to that of Figure 6 of Vilhu & Walter (1987). F89 instead found a significant number of K ($B-V \geq 0.9$) and M stars ($B-V \geq 1.4$) with fractional surface fluxes as high as $\sim 10^{-2.5}$. Slightly more than half their sample of late-type stars with determined v sin i-values were type K or M. We have a comparable fraction of K and M stars (although far fewer M stars relative to K stars; Table 7). But we should also note that the Slew in its current form is incomplete for spectral types K and M (see § 3.6). When complete, it might have significantly more $F_X/F_{bol} > 10^{-3}$ stars than it does now (possibly due to flaring).

3.5. *Slope of the L_X–v sin i Relation in Single Stars*

Earlier we showed that the basic correlation in the data on all three single star samples is between R and L_X (Tables 9A–9D). However, for comparison with previous studies, we determined the apparent slope of the L_X–v sin i relation in the Slew and Slew+F89 samples. Unfortunately, v sin i upper limits must be excluded from any regression analysis (see below).

Results of our linear regression work are provided in Tables 9A–9D, and in Figures 6*a* (for the Slew sample) and 6*b* (for the combined). To evaluate the goodness of fit, we used two tests. First, we used a standard least-squares χ^2 analysis, propagating the errors in the Slew fluxes to errors in L_X.[12] Second, as both the Slew and combined datasets have many outlier points, we used the absolute deviation instead of χ^2 as the merit function (minimizing the absolute value of the deviations, rather than their square). In both cases, and with both datasets, the merit function is significantly larger than the number of degrees of freedom, implying that a single spectral slope is unacceptable.

From Figure 6*a*, we see that the largest residuals to the best-fit line are concentrated at higher values of v sin i, namely at rotation speeds higher than the median of 13.0 km s^{-1}. Also, the functional forms of the best-fit line and that from Pallavicini et al. (1982) are nearly identical. Turn now to Figure 6*b*. Here the data at high v sin i-values appear to demand a *flattening* in the L_X–v sin i relation, although at low v sin i-values the quadratic behavior is acceptable. The distribution of L_X for the higher than median (v sin $i > 15.6$ km s^{-1}) group of the combined Slew+F89 sample is clearly weighted toward lower values of L_X than would be expected if a quadratic slope applied (Figs. 7*a* and 7*b*).

We caution that the F89 sample is biased toward higher v sin i for a given value of L_X than the Slew—a reflection of their adopted uniform upper limit of less than 10 km s^{-1} for v sin i nondetections.

By analogy with the foregoing correlation analysis, one might think that including the Slew or EMSS upper limits in the analysis would improve the fit, as these quantities do provide some information. However, standard packages such as ASURV are unable to perform regression analysis on data like these, as the upper limits are nonrandomly distributed in the data space.[13] They instead only occur for small values of v sin i (*Type 1 Censoring*). Further, the only way to treat upper limits in the independent variable in a least-squares fit is to use Schmitt's binned Kaplan-Meier method (Schmitt 1985). But the Kaplan-Meier estimator of the EMSS v sin i distribution has all the upper limits (more than half the data points) in a single bin, and so it is clearly not amenable to this treatment. The K–M estimators of the Slew, and of the combined (Slew+F89) distributions, are less extreme, but the Slew, F89, and combined v sin i distributions (in ASURV) put all the upper limits into the first few bins. Regression of samples with extreme Type 1 censoring has not been widely studied, and further work in this area (e.g., Marshall 1994) is therefore necessary.

[12] Distance errors (in the parallax, or in the observed values of B and V) have been ignored in this analysis. Including them gives a slope to the L_X–v sin i relation of 2.13 ± 0.07 with χ^2/dof = 273/28 for the Slew sample. These results are similar to those in Table 9A.

[13] We note that F89 included the upper limits in the fit by the *Ansatz* of redefining them to be detections of 5 ± 5 km s^{-1}. We regard this as suspect.

© American Astronomical Society • Provided by the NASA Astrophysics Data System

1996ApJ...463..747S

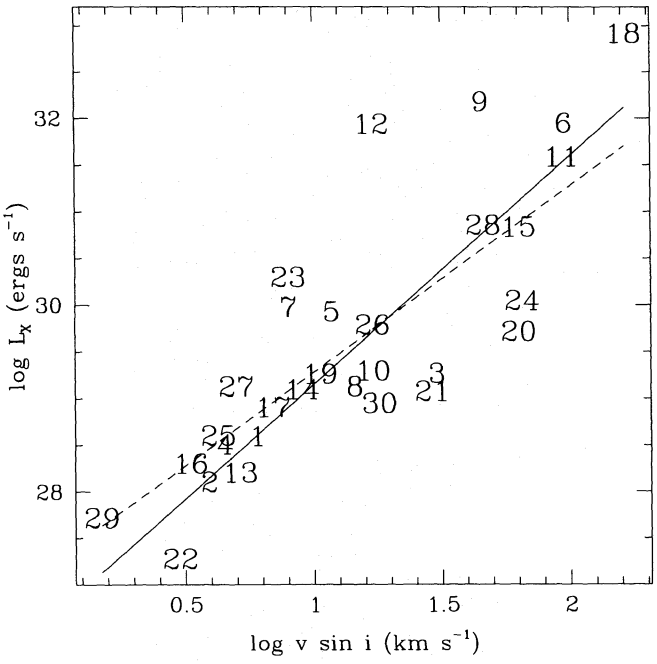

FIG. 6a

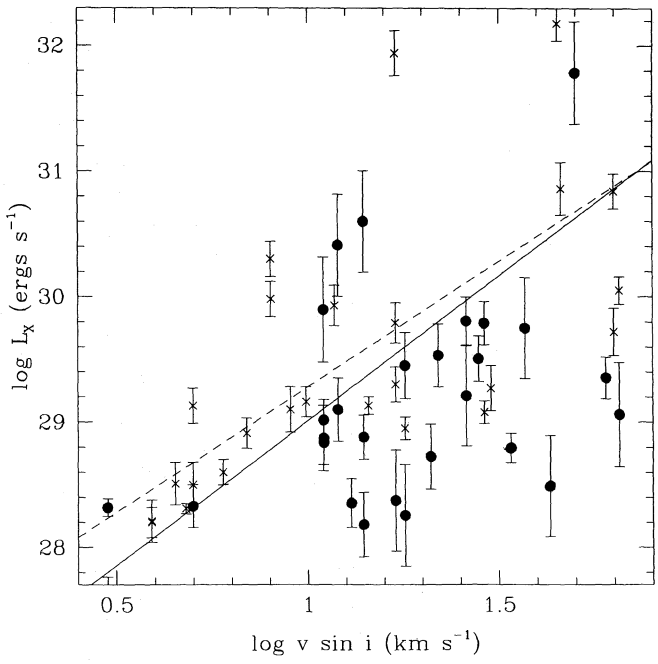

FIG. 6b

FIG. 6.—L_X vs. v sin i relation for (*a*) all F7–M5 Slew single star points with detected v sin i's, numbers corresponding to part A of Table 7, compared with least-squares best-fit line (*solid line*) and Pallavicini et al. (1982) optically selected sample quadratic line (*dotted line*); and (*b*) the combined sample of single F7–M5 stars with detected v sin i's from this paper (part A of Table 7, *crosses*) and the EMSS (F89, *points*) line notation as in (*a*). In (*a*), the numeric labels for five stars have been displaced slightly to enhance readability: 16 and 25 upward and to the left; 2 and 13 downward; and 19 upward. For both (*a*) and (*b*), the explicit forms of the best-fitting lines are given in Tables 9A–9D. The Pallavicini et al. line is log $L_X = 27.28 + 2.0$ log (v sin i).

3.6. *Group Properties*

We close by discussing the group properties of the Slew stars. Of the 229 stars identified to date in the Slew, the fractional content of B, F, and G stars normalized to all stars of types B–M (excluding A stars) agrees well within the errors with the GPX and EMSS stellar samples (Slew: 45% ± 4%, GPX: 51% ± 9%, EMSS: 51% ± 3%). Because the identified portion of the Slew is known to be incomplete for spectral types later than G (or $V \sim 8$; see § 2), the relative numbers of K and M stars are expected to increase slightly when the currently unidentified 10% of the survey is fully studied.

We can also estimate the number of expected new K and M stars. Some 26% of the *identified* high latitude ($|b_{II}| > 20°$) Slew sources are stellar, which agrees well with the

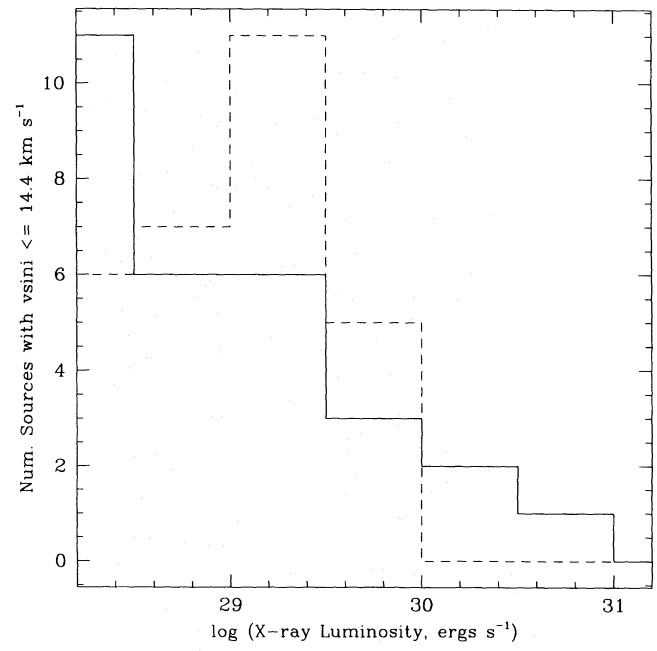

FIG. 7a

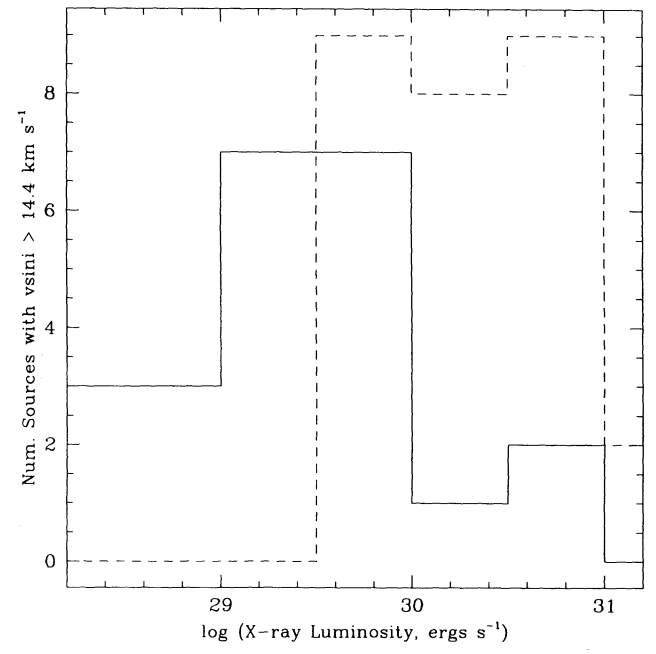

FIG. 7b

FIG. 7.—Luminosity distributions for low [≤ 15.6 km s^{-1}; (*a*)] and high v sin i (*b*) for F89+Slew F7–M5 single stars with detected v sin i's (*solid histograms*) are compared with distributions expected from Pallavicini et al. (1982), with the observed v sin i-values (*dashed histograms*).

© American Astronomical Society • Provided by the NASA Astrophysics Data System

1996ApJ...463..747S

EMSS. By comparison, the GPX is 43% stellar, probably because it contains more disk stars, which are more likely to be young and active. The total stellar content of the Slew (at all latitudes) when fully identified would be expected to be somewhere in between the GPX and EMSS results, or ~35%. This implies ~50 new stellar IDs in the unidentified sources, mostly K and M stars. This result is consistent with an alternate approach using X-ray to optical ratios from the EMSS and the known completeness of stellar catalogs.

4. SUMMARY

The properties of stellar sources in the *Einstein* Slew Survey have been discussed. The main points are as follows:

1. For 63 cool stars (A–M stars in part A of Table 1), the Slew Survey provides the first ever X-ray detection.

2. There was one case of extreme youth, 1ES 1354−314 (=HD 121688; $v \sin i = 63$ km s^{-1}).

3. An A-star candidate, 1ES 1126−610, may be an X-ray source (subject to confirmation by our HRI observations).

4. Four unexpected, unusual stellar X-ray counterparts have been optically identified with Slew sources: two T Tauri stars (1ES 0638+094 and 1ES 0625−600), and two new cataclysmic variables (1ES 0437−046 = BF Eri, and 1ES 1536+515). One additional source, 1ES 1841−044, is likely to be a newly discovered accretion-powered object, because of the extreme f_X/f_V ratio.

5. For the 22 single F7–M5 Slew stars with measured values of rotational velocity ($v \sin i$; including upper limits with ASURV) we find a 99.9% confidence level correlations of L_X with either $v \sin i$ or stellar radius (R). A reanalysis of the corresponding subset of EMSS stars, again including upper limits, confirms the published result that only L_X and R are correlated. A combined sample, formed by simply adding together the EMSS and Slew single F7–M5 stars, gives 99.9% L_X–$v \sin i$ and L_X-R correlations.

6. We find a correlation between L_X and Rossby number (R_0) at more than 99% confidence in the Slew single F7–M5 stars, and that $L_X \propto R_0^{-0.4}$ is equivalent to $L_X \propto (v \sin i)^{0.4}$. The single stars with $B-V > 0.6$ appear to have a maximum efficiency for producing X-rays given by $F_X/F_{bol} = 10^{-3}$. Quasi-quadratic slopes to the L_X–$v \sin i$ data are acceptable for low rotation speeds (<14 km s^{-1}); however, at higher $v \sin i$-values, the Slew data alone shows considerable scatter. The combined Slew+EMSS data demand a flattening of the L_X–$v \sin i$ relation for high rotation speeds. All of these results are expected if there is saturation of the stellar surface with active regions at high L_X.

7. We expect ~50 new stellar identifications in the unidentified Slew survey source set (currently 93% identified for $b_{II} > 20°$).

This work was supported by NASA grants NAG5–1746 (Slew ADP), and NAG5–2104 (*ROSAT*) to the Smithsonian Astrophysical Observatory. S. S. and M. B. acknowledge partial support from MURST, GNA-CNR, and ASI. We thank J. Huchra and the SAO Tillinghast observers for obtaining a spectrum of 1ES 1536+515. J. S. acknowledges useful conversations with L. Golub and J. Bookbinder, and is grateful to T. Lerner for her help in assembling the rotational velocity data from the literature. S. H. S. wishes to thank NSO for a generous allotment of observing time, the McMath-Pierce stellar spectrograph team for their help, and I. Szegvari for help with the data analysis. This research has made use of the SIMBAD database, operated at CDS, Strasbourg, France.

REFERENCES

Allen, C. W. 1975, Astrophysical Quantities (3d ed.; London: Athlone), 205
Balachandran, S. 1990, ApJ, 354, 310
Barbera, M., Micela, G., Sciortino, S., Harnden, F. R., Jr., & Rosner, R. 1993, ApJ, 414, 846
Becker, R. H., White, R. L., & Edwards, A. L. 1991, ApJS, 75, 1
Benz, W., & Mayor, M. 1984, A&A, 138, 183
Bernacca, P. L., & Perinotto, M. 1973, Contr. Oss. Af. Padova Asiago, 239, 250
Bolton, C. T., Aslan, Z., Kamper, K. W., & Lyons, R. W. 1981, AJ, 86, 1267
Bonneau, D., Blazit, A., Foy, R., & Labeyrie, A. 1980, A&AS, 42, 185
Breen, J., Raychaudhury, S., Forman, W., & Jones, C. 1994, ApJ, 424, 59
Brunet, J. P., Imbert, N., Martin, N., Mianes, P., Prevot, L., & Rebeirot, E., & Rousseau, J. 1975, A&AS, 21, 109
Caillault, J. P., & Helfand, D. 1985, ApJ, 289, 279
Cash, W., & Snow, T. P., Jr. 1982, ApJ, 263, L59
Cayrel de Strobel, G., & Cayrel, R. 1989, A&A, 218, L9
Chlebowski, T., Harnden, F. R., Jr., & Sciortino, S. 1989, ApJ, 341, 427
Corbally, C. J. 1984, ApJ, 285, 195
Coyne, G. V., & MacConnell, D. J. 1983, Vatican Obs. Publ., 2(6), 73
Damiani, F., Micela, G., Sciortino, S., & Harnden, F. R., Jr. 1994, ApJ, 436, 807
Donati, J.-F., Henry, G. W., & Hall, D. S. 1995, A&A, 293, 107
Drake, S. A. 1993, private communication
Drake, S. A., Linsky, J. L., Schmitt, J. H. M. M., & Rosso, C. 1994a, ApJ, 420, 387
Drake, S. A., Simon, T., & Linsky, J. L. 1989, ApJS, 71, 905
———. 1992, ApJS, 82, 311
Drake, S. A., Simon, T., Linsky, J. L., & White, N. 1994b, in ASP Conf. Ser. 64, Cool Stars, Stellar Systems, and the Sun, ed. J.-P. Caillault (San Francisco: ASP), 690
Duncan, D. K., Baliunas, S. L., Noyes, R. W., Vaughan, A. H., Frazer, J., & Lanning, H. H. 1984, PASP, 96, 707
Duncan, D. K., Wilson, O. C., Preston, G. W., Frazer, J., & Vaughan, A. H. 1991, ApJS, 76, 383
Eaton, J. A. 1990, IAU Inf. Bull. Var. Stars, 3460, 1
Elvis, M., Plummer, D., Schachter, J., & Fabbiano, G. 1992, ApJS, 80, 257
Favata, F., Barbera, M., Micela, G., & Sciortino, S. 1995, A&A, 295, 147
Fleming, T. A., Gioia, I. M., & Maccacaro, T. 1989, ApJ, 340, 1011
Gilman, P. A. 1982, in Cool Stars, Stellar Systems, and the Sun, Vol. 1, ed. M. Giampapa & L. Golub (SAO Spec. Rep. 392), 165
Glebocki, R., Musielak, G., & Stawikowski, A. 1980, Acta Astron., 30(4), 453
Golub, L., Harnden, F. R., Jr., Maxson, C. W., Rosner, R., Vaiana, G. S., Cash, W., Jr., & Snow, T. P., Jr. 1983, ApJ, 271, 264; 278, 456
Goraya, P. S., & Rautela, B. S. 1985, Ap&SS, 113, 373
Gray, D. F. 1988, Lectures on Spectral Line Analysis: F, G, and K Stars (Arva: The Publisher)
———. 1984, ApJ, 281, 719
Gray, D. F., Baliunas, S. L., Lockwood, G. W., & Skiff, B. A. 1992, ApJ, 400, 681
Gray, D. F., & Nagar, P. 1985, ApJ, 298, 756
Griffin, R. F., Mayor, M., & Gunn, J. E. 1982, A&A, 106, 221
Grillo, F., Sciortino, S., Micela, G., Vaiana, G. S., & Harnden, F. R., Jr. 1992, ApJS, 81, 795
Haisch, B., Schmitt, J. H. M. M., & Rosso, C. 1991, ApJ, 383, L15
Hamann, F., & Persson, S. E. 1992, ApJS, 82, 247
Harnden, F. R., Jr. 1992, ApJ, 391, 667
Harnden, F. R., Jr., et al. 1979, ApJ, 234, 51
Hartkopf, W. I., & McAlister, H. A. 1984, PASP, 96, 105
Hempelmann, A., Schmitt, J. H. M. M., Schultz, M., Rüdiger, G., & Stepien, K. 1995, A&A, 294, 515
Hertz, P., & Grindlay, J. E. 1988, AJ, 96(1), 233
Hoffleit, D., & Jaschek, C. 1982, The Bright Star Catalogue (4th rev. ed.; New Haven: Yale Univ. Obs.)
Huenemoerder, D. P., Ramsey, L. W., Buzasi, D. L., & Nations, H. L. 1993, ApJ 404, 316
Huenemoerder, D. P. 1986, AJ, 92, 673
Jeffries, R. D. 1995, MNRAS, 273, 559
Joncour, I., Bertout, C., & Menard, F. 1994, 285, L25
Kashyap, R., Rosner, R., Micela, G., Sciortino, S., Vaiana, G. S., & Harnden, F. R., Jr. 1992, ApJ, 391, 667
Kuerster M., Schmitt, J. H. M. M., & Cutispoto, G. 1994, A&A, 289, 899
Linsky, J. L. 1985, Sol. Phys., 100, 333
———. 1990, in Imaging X-Ray Astronomy, ed. M. Elvis (Cambridge: Cambridge Univ. Press), 39
———. 1993, in Physics of Solar and Stellar Coronae, ed. J. Linsky & S. Serio (Noordwijk: Kluwer), 257
Linsky, J. L., Andrulis, C., Saar, S. H., Ayres, T. R., Giampapa, M. S. 1994, in ASP Conf. Ser. 64, Cool Stars, Stellar Systems, and the Sun, ed. J.-P. Caillault (San Francisco: ASP), 438

© American Astronomical Society • Provided by the NASA Astrophysics Data System

1996ApJ...463..747S

Linsky, J. L., Drake, S. A., & Bastian, T. S. 1992, ApJ, 393, 341
Long, K. S., & White, R. L. 1980, ApJ, 239, L65
Maggio, A., Vaiana, G. S., Haisch, B. M., Stern, R. A., Bookbinder, J., Harnden, F. R., Jr., & Rosner, R. 1990, ApJ, 348, 253
Mahmoud, F. M. 1993, Ap&SS, 209, 237
Marcy, G. W., & Chen, G. H. 1992, ApJ, 390, 550
Marshall, H. L. 1994, in ASP Conf. Ser. 61, Astronomical Data Analysis Software and Systems III, ed. D. R. Crabtree, R. J. Hanisch, & J. Barnes (San Francisco: ASP), 403
Micela, G., Sciortino, S., & Serio, S. 1985a, in X-Ray Astronomy 1984, ed. M. Oda & R. Giacconi (Tokyo: ISAS), 43
Micela, G., Sciortino, S., Serio, S., Vaiana, G. S., Bookbinder, J., Golub, L., Harnden, F. R., Jr., & Rosner, R. 1985b, ApJ, 292, 172
Micela, G., Sciortino, S., Vaiana, G. S., Harnden, F. R., Jr., Rosner, R., & Schmitt, J. H. H. M. 1990, ApJ, 348, 557
Mihalas, D., & Binney, J. 1981, Galactic Astronomy: Structure and Kinematics (2d ed.; San Francisco: Freeman)
Niarchos, P. G. 1987, A&AS, 67, 365
Noyes, R. W., Hartmann, L. W., Baliunas, S. L., Duncan, D. K., & Vaughan, A. H. 1984, ApJ, 279, 763
Osten, R. A., & Saar, S. H. 1996, in preparation
Pallavicini, R. 1989, Astron. Astrophys. Rev., 1, 177
Pallavicini, R., Golub, L., Rosner, R., Vaiana, G. S., Ayres, T. R., & Linsky, J. L. 1981, ApJ, 248, 279
Pallavicini, R., Golub, L., Rosner, R., & Vaiana, G. 1982, in Cool Stars, Stellar Systems, and the Sun, ed. M. S. Giampapa & L. Golub (SAO Spec. Rep. 392), II-77
Pan, K.-K., Tan, H.-S., Wang, X.-H., Zhao, Z.-W., Xu, J., & Cha, G.-W. 1992, Acta Astrophys. Sinica, 33, 395
Pannunzio, R., & Morbidelli, R. 1984, A&AS, 55, 455
Pasquini, L., & Pallavicini, R. 1991, A&A, 251, 199
Pasquini, L., Pallavicini, R., & Dravins, D. 1989, A&A, 213, 261
Perlman, E. S., et al. 1996, ApJ, 104, in press
Petersen, B. R. 1980, PASP, 92, 188
Piirola, V., & Vilhu, O. 1982, A&A, 110, 351
Piskunov, N. E., Tuominen, I., Vilhu, O. 1990, A&A 230, 363
Plummer, D., Schachter, J., Garcia, M., Elvis, M., & McDowell, J. 1994, CD-ROM (Cambridge: SAO)
Pounds, K. A., et al. 1993, MNRAS, 260, 77
Press, W. H., Flannery, B. P., Teukolsky, S. A., & Vetterling, W. T. 1986, Numerical Recipes (Cambridge: Cambridge Univ. Press)
Radick, R. R., Thompson, D. T., Lockwood, G. W., Duncan, D. K., & Bagget, W. E. 1987, ApJ 321, 459
Randich, S., Giampapa, M. S., & Pallavicini, R. 1994, A&A, 283, 893
Remillard, R., et al. 1996, in preparation
Robertson, T. H., & Hamilton, J. E. 1987, AJ, 93, 959
Rosner, R., Golub, L., & Vaiana, G. S. 1985, ARA&A, 23, 413
Rosner, R., & Vaiana, G. S. 1980, in X-Ray Astronomy, ed. R. Giacconi & G. Setti (Dordrecht: Reidel), 129
Ruciński, S. M., & Vandenberg, D. A. 1986, PASP, 98, 669
Saar, S. H. 1991, in IAU Colloq. 130, The Sun and Cool Stars: Activity, Magnetism, Dynamos, ed. I. Tuominen, D. Moss, & G. Rüdiger (Berlin: Springer), 389
Saar, S. H., & Baliunas, S. L. 1992, in ASP Conf. Ser. 27, The Fourth Solar Cycle Workshop, ed. K. L. Harvey (San Francisco: ASP), 197
Saar, S. H., Linsky, J. L., & Beckers, J. M. 1986, ApJ 302, 777
Saar, S. H., Nordström, B., & Andersen, J. 1990, A&A, 235, 291
Schachter, J. F., & Elvis, M. 1996, in preparation
Schachter, J., et al. 1993, ApJ, 412, 541
Schachter, J. F., Elvis, M., & Voges, W. 1993, in ASP Conf. Ser. 51, Observational Cosmology, ed. G. Chincarini, A. Iovino, T. Maccacaro, & D. Macagni (San Francisco: ASP), 475
Schmitt, J. H. M. M. 1985, ApJ, 293, 178
———. 1990, Adv. Space Res., 10, 115
Schmitt, J. H. M. M., Collura, A., Sciortino, S., Vaiana, G. S., Harnden, F. R., Jr., & Rosner, R. 1990, ApJ, 365, 704
Schmitt, J. H. M. M., Golub, L., Harnden, F. R., Jr., Maxson, C. W., Rosner, R., & Vaiana, G. S. 1985, ApJ, 290, 307
Schmitt J. H. M. M., Zinnecker, H., Cruddace R., & Harnden, F. R., Jr. 1992, ApJ, 402, 13
Schmitt, J. H. M. M., Zinnecker, H., Cruddace, R., & Harnden, F. R., Jr. 1993, ApJ, 402, L13
Sciortino, S. 1993, in Physics of Solar and Stellar Coronae, ed. J. Linsky & S. Serio (Dordrecht: Kluwer), 211
Sciortino, S., Favata, F., & Micela, G. 1993, A&A, in press
Sciortino, S., Vaiana, G. S., Morossi, C., Ramella, M., Harnden, F. R., Jr., Schmitt, J. J. M. M., & Rosner, R. 1990, ApJ, 220, 361
Slane, P. O., et al. 1996, ApJ, submitted
Soderblom, D. R., Pendleton, J., & Pallavicini, R. 1989, AJ, 97, 5
Stauffer, J. R., & Hartmann, L. W. 1986, ApJS, 61, 531
Stauffer, J. R., Giampapa, M. S., Herbst, W., Vincent, J. M., Hartmann, L. W., & Stern, R. A. 1991, ApJ, 374, 142
Stauffer, J. R., et al. 1994, ApJS, 91, 625
Stern, R. A., Schmitt, J. H. M. M., Rosso, C., Pye, J. P., Hodgkin, S. T., & Stauffer, J. R. 1992, ApJ, 399, 159
Stocke, J. T., Morris, S. L., Gioia, I. M., Maccacaro, T., Schild, R., Wolter, A., Fleming, T. A., & Henry, J. P. 1991, ApJS, 76, 813
Strassmeier, K. G., Fekel, F. C., Bopp, B. W., Dempsey, R. C., & Henry, G. W. 1990, ApJS, 72, 191
Strassmeier, K. G., Hall, D. S., Zeilik, M., Nelson, E., Eker, Z., & Fekel, F. C. 1988, A&AS, 72, 291
Strassmeier, K. G., Rice, J. B., Wehlau, W. H., Hill, G. M., & Matthews, J. M. 1993, A&A, 268, 671
Torres, C. A. O., Busko, I. C., & Quast, G. R. 1983, IAU Colloq. 71, Activity in Red-Dwarf Stars, ed. P. Byrne & M. Redono (Dordrecht: Reidel), 175
Uesugi, A., & Fukuda, I. 1970, Contr. Astroph. Kwasan Obs. Univ. Kyoto, 189, 205
Ulmschneider, P. 1990, in Proc. 6th Cambridge Workshop, Cool Stars, Stellar Systems, and the Sun, ed. G. Wallerstein (San Francisco: ASP), 3
Vaiana, G. S. 1990, in Imaging X-ray Astronomy, ed. M. Elvis (Cambridge: Cambridge Univ. Press), 227
Vaiana, G. S., et al. 1981, ApJ, 245, 163
Vaiana, G. S., Maggio, A., Micela, G., & Sciortino, S. 1992, Mem. Soc. Astron. Italiana, 63, 545
Vaughan, A. H., Preston, G. W., & Wilson, O. C. 1978, PASP, 90, 267
Vilhu, O. 1987, in Cool Stars, Stellar Systems, and the Sun, ed. J. L. Linsky & R. E. Stencel (Dordrecht: Reidel), 110
Vilhu, O., & Walter, F. M. 1987, ApJ, 321, 958
Walter, F. M., et al. 1987, A&A, 314, 297
Walter, F. M., Bowyer, C. S., Linsky, J. L., & Garmire, G. 1980a, ApJ, 236, L137
Walter, F. M., Cash, W., Charles, P. A., & Bowyer, C. S. 1980b, ApJ, 236, 212
Zinnecker, H., & Preibisch, T. 1995, Ap&SS, 224, 587

Note added in proof.—S. Drake has recently pointed out to us that 1ES 0712−363 (=HD 56142) and 1ES 2052−172 (=HD 199143; not in the 819 source list described in § 2.5) were detected in VLA observations and hence are candidate RS CVn systems (§ 2.4).

© American Astronomical Society • Provided by the NASA Astrophysics Data System